

Behaviour of Low-Rise Shear Walls with Hybrid GFRP-Steel  
Reinforcement and Steel Fibre-Reinforced Concrete

by

Sina Ghazizadeh

A thesis submitted in partial fulfillment of the requirements for the  
degree of

Master of Science

in

Structural Engineering

Department of Civil and Environmental Engineering  
University of Alberta

© Sina Ghazizadeh, 2017

## ABSTRACT

Recent earthquakes have revealed that conventional steel-reinforced concrete (RC) shear walls can exhibit considerable damage and residual displacements even after moderate intensity earthquakes. These residual displacements can result in high post-earthquake repair costs. Recent advances in the science of composite materials have motivated the search for cost-efficient solutions to improve seismic behaviour of low-rise walls.

This study investigates the potential of fibre-reinforced polymer (FRP) bars and fibre-reinforced concrete (FRC) to improve the behaviour of low-rise walls. Use of hybrid vertical reinforcement consist of steel and GFRP bars is proposed. The steel lends ductility to the system, while the elastic behaviour of GFRP material enhances the self-centering ability of the wall to reduce residual displacements.

First, using a preliminary finite-element (FE) analysis model, a parametric study was conducted to determine the most suitable hybrid scheme in terms of ductility, stiffness, strength and self-centering. Performance of the hybrid system subjected to earthquake loading was studied using a simplified nonlinear dynamic analysis. The response of RC and hybrid FRP-steel walls were shown to be comparable when designed properly in terms of stiffness and serviceability.

To verify the modeling results, two low-rise concrete shear walls with similar geometry were built and tested up to failure under pseudo-static lateral cyclic loading. First wall was a conventional steel-reinforced concrete (RC) shear wall with height-to-length ratio of 1, designed as per the seismic considerations of CSA A23.3-14 and ACI 318-14 codes with a relaxation in confinement reinforcement. The second was an innovative wall with hybrid GFRP-steel vertical reinforcement and steel fibre-reinforced concrete (SFRC). The SFRC was used to mitigate the damage

experienced by the concrete. This design also provides the opportunity to evaluate potential of SFRC for confinement relaxation in shear walls suggested in the literature.

Then the FE model was improved to capture the test results by including bond-slip mechanism and buckling of the reinforcing bars in the analyses. The model was shown to be able to predict system performance variables with satisfactory accuracy for both walls, such as strength, stiffness, and self-centering. The effect of several reinforcement arrangement in low-rise walls was investigated using the analysis model and the advantages of hybrid system over exclusively FRP-reinforced and steel-reinforced walls were discussed.

It is shown that in hybrid FRP-steel low-rise walls, an arrangement of FRP bars at the middle region of the wall together with steel bars at the wall boundaries is able to achieve comparable strength, stiffness and ductility with conventional RC walls. The hybrid system has improved self-centering behaviour in comparison to its RC counterpart, while maintaining a significant energy dissipation capacity. Backbone curve of force-displacement response of a hybrid wall shows a characteristic tri-linear behaviour, which is not associated with capacity deterioration. The developed model can be used to provide a better understanding of the performance of the hybrid system at the material and system levels. Addition of fibres increases post-cracking damage tolerance of the wall, but do not delay buckling of longitudinal bars. Some potential of steel fibre-reinforced concrete to increase ductility of low-rise walls are discussed using the developed model.

## **PREFACE**

This thesis is an original work by the author, Sina Ghazizadeh.

Chapter 2 of this thesis has been submitted to journal of Engineering Structures as Ghazizadeh, S., Cruz-Noguez, C., and Talaei, F. “ANALYTICAL MODEL FOR HYBRID FRP-STEEL REINFORCED SHEAR WALLS” in November 2016. Validation of GFRP-reinforced shear walls was provided by the third author, Fereshte Talaei. Supervision and revisions of Dr. Carlos Cruz-Noguez, the second author, is greatly appreciated.

A version of chapter 3 has been submitted to Journal of Composites for Construction as Ghazizadeh, S. and Cruz-Noguez, C. “DAMAGE-RESISTANT CONCRETE LOW-RISE SHEAR WALLS WITH HYBRID GFRP-STEEL REINFORCEMENT AND STEEL FIBRES” in March 2017. Dr. Carlos Cruz-Noguez was the supervisory author and was involved with concept formation and manuscript composition.

Chapter 4 has not been submitted yet.

*Dedicated with love to my family*

## **ACKNOWLEDGEMENT**

First and foremost, I would like to thank merciful God for what I have achieved in my life.

Financial support for this research was provided through a Discovery Grants program by the Natural Sciences and Engineering Research Council of Canada (NSERC). Required concrete for the walls was donated by Lafarge North America. Technical expertise and material support from BP Automation, Harris Rebar, and Superior Lumber from Edmonton, Canada, are gratefully acknowledged.

I would like to express my gratitude to my supervisor Dr. Carlos Cruz-Noguez for his patience, guidance, support and encouragement during the project. I have learned many valuable things by working with him. The assistance of the technicians of I.F. Morrison Structures Laboratory, Greg Miller and Cameron West, and fellow graduate student, Mohammad Javad Tolou Kian, to the success of the experimental program is gratefully acknowledged.

Last but not least, I would like to extend my sincere gratitude to my parents and brother for the continued love and care they have provided throughout my life. In addition, many thanks to my friends and relatives here in Edmonton and back in Iran who supported me mentally during this journey.

# TABLE OF CONTENTS

<b>ABSTRACT</b> .....	ii
<b>PREFACE</b> .....	iv
<b>ACKNOWLEDGEMENT</b> .....	vi
<b>TABLE OF CONTENTS</b> .....	vii
<b>LIST OF TABLES</b> .....	x
<b>LIST OF FIGURES</b> .....	xi
<b>CHAPTER 1 INTRODUCTION</b> .....	1
1.1 Background .....	1
1.2 Research Obejectives .....	3
1.3 Methodology .....	3
<b>CHAPTER 2 ANALYTICAL MODEL FOR HYBRID FRP-STEEL REINFORCED SHEAR WALLS</b> .....	5
2.1 Introduction .....	5
2.2 Analysis Model for GFRP-Reinforced Shear Walls .....	6
2.3 Analysis Model for hybrid GFRP-Steel Reinforced Shear Walls.....	7
2.3.1 Design aspects .....	8
2.3.2 Wall models.....	8
2.3.3 Results and discussion .....	10
2.3.3.1 Ultimate strength.....	12
2.3.3.2 Failure mode .....	12
2.3.3.3 Displacement capacity .....	12
2.3.3.4 Self-centering.....	13
2.3.3.5 Energy dissipation.....	14
2.3.3.6 Serviceability .....	14
2.3.4 Seismic behaviour.....	15

2.4 Conclusions .....	20
<b>CHAPTER 3 DAMAGE-RESISTANT REINFORCED CONCRETE LOW-RISE WALLS WITH HYBRID GFRP-STEEL REINFORCEMENT AND STEEL FIBRES .....</b>	<b>22</b>
3.1 Introduction .....	22
3.2 Experimental Program.....	24
3.2.1 Design and details of specimens.....	24
3.2.2 Material properties.....	26
3.2.3 Instrumentation, test setup, and loading protocol.....	27
3.3 Experimental Results.....	29
3.3.1 Hysteretic load-displacement response, strength, and stiffness .....	29
3.3.2 Damage progression and failure mode .....	32
3.3.2.1 First cracking .....	32
3.3.2.2 Flexural-shear cracks .....	32
3.3.2.3 Reinforcement yielding.....	32
3.3.2.4 Post-cracking stage and major damages .....	33
3.3.2.5 Buckling of longitudinal bars.....	34
3.3.3 Self-centering and energy dissipation capacity .....	35
3.3.4 Strains in longitudinal reinforcement .....	36
3.4 Conclusions .....	38
<b>CHAPTER 4 NUMERICAL MODELING OF REINFORCED CONCRETE LOW-RISE WALLS WITH HYBRID GFRP-STEEL VERTICAL REINFORCEMENT AND STEEL FIBRES .....</b>	<b>40</b>
4.1 Introduction .....	40
4.2 Summary of Experimental Program.....	42
4.3 Analysis Model for Steel-Reinforced Concrete Walls.....	43
4.3.1 Constitutive materials and model development.....	43
4.3.2 Model validation.....	45

4.4 Analysis Model for Hybrid FRP-Steel Reinforced Concrete Walls .....	48
4.4.1 Constitutive materials and model development.....	48
4.4.2 Model validation.....	48
4.5 Parametric Study .....	50
4.5.1 FRP reinforcement.....	50
4.5.1 Steel fibre-reinforced concrete (SFRC).....	53
4.6 Conclusions .....	59
<b>CHAPTER 5 SUMMARY, CONCLUSIONS AND FUTURE WORK.....</b>	<b>61</b>
<b>REFERENCES.....</b>	<b>63</b>

## LIST OF TABLES

Table 2.1. Summary of analysis results for different models .....	12
Table 2.2 Results of seismic analysis .....	18
Table 4.1. Summary of modeling results for the control wall .....	46
Table 4.2. Summary of modeling results for the hybrid and GFRP-reinforced models .....	52

## LIST OF FIGURES

Fig. 2.1. GFRP-reinforced shear walls (mohamed, 2013) .....	7
Fig. 2.2. Calculated vs. measured response for wall G12.....	7
Fig. 2.3. Reinforcement detail of the models.....	9
Fig. 2.4. Wall A model and loading protocol .....	11
Fig. 2.5. Calculated base shear vs. top displacement responses .....	11
Fig. 2.6. Typical definition of idealized force-displacement envelope and yield displacement...	13
Fig. 2.7. Envelope of hysteretic response in wall A, C, and F.....	15
Fig. 2.8. Earthquake acceleration records (PEER, 2016), and calculated response spectral accelerations .....	16
Fig. 2.9. Hysteretic model for wall A .....	17
Fig. 2.10. Displacement and base shear histories for mass of $1700 \times 10^3$ kg.....	19
Fig. 3.1. Reinforcement details of specimens .....	25
Fig. 3.2. Material properties.....	27
Fig. 3.3. Bracing frame .....	28
Fig. 3.4. Preparation and lifting .....	28
Fig. 3.5. Instrumentation.....	28
Fig. 3.6. Loading protocol and the hydraulic actuator.....	29
Fig. 3.7. Lateral load vs. top displacement response of the walls.....	30
Fig. 3.8. Backbone curves of the hysteretic responses .....	31
Fig. 3.9. Secant stiffness of the walls.....	32
Fig. 3.10. Crack pattern and damage progression.....	34
Fig. 3.11. Toe of the walls after bars buckling .....	35
Fig. 3.12. Residual displacements of hysteretic cycles.....	36
Fig. 3.13. Energy dissipation capacity through hysteretic cycles .....	36
Fig. 3.14. Tensile strains of outermost reinforcement .....	37
Fig. 3.15. Strains at the base of GFRP bars .....	38
Fig. 3.16. Neutral axis depth.....	38
Fig. 4.1. Reinforcement details of specimens .....	43

Fig. 4.2. Material properties in the tests and models .....	43
Fig. 4.3. Loading protocol and one of the models .....	45
Fig. 4.4. Mesh sensitivity analysis results.....	45
Fig. 4.5. Force-displacement response of the control wall models.....	46
Fig. 4.6. Concrete crushing at compressed toe .....	47
Fig. 4.7. Force-displacement response of HW-M1 and HW-M2 models.....	49
Fig. 4.8. Tensile strains at the base of GFRP bars .....	49
Fig. 4.9. Detailing of the hybrid and GFRP-reinforced models.....	51
Fig. 4.10. Force-displacement response of the hybrid and GFRP-reinforced models.....	52
Fig. 4.11. Detailing of Trial5 and Trial6 models .....	54
Fig. 4.12. Force-displacement response of Trial5 and Trial6 models .....	54
Fig. 4.13. Detailing and concrete behaviour of Trial7 and Trial8 models.....	55
Fig. 4.14. Force-displacement response of Trial7 and Trial8 models with and without fibres ....	55
Fig. 4.15. Force-displacement response of hybrid wall with 60 MPa SFRC.....	57
Fig. 4.16. Force-displacement response of the walls under different axial loads.....	58
Fig. 4.17. Probability of having to demolish a building (Ramirez and Miranda, 2012).....	59

# CHAPTER 1 INTRODUCTION

## 1.1 Background

In reinforced-concrete (RC) structures, shear wall elements have a dual role of resisting both the gravity and lateral loads. Providing high in-plane stiffness and strength to the structure, shear walls show to be a cost-efficient and reliable solution for drift control and resisting seismic loads (Mohamed, 2013). Shear walls can be found in various shapes and sizes, commonly with rectangular cross-section. The configuration usually complies with building architectural plan, while the geometry and dimensions of the wall affect its strength, stiffness and ductility considerably (Athanasopoulou, 2010).

One of the most common classifications of structural walls is according to their height-to-length ratio (aspect ratio). Walls with an aspect ratio smaller than two are typically known as low-rise or squat walls in North America. Shear behaviour is significant in the response of low-rise walls under lateral loads. These nonlinear shear deformations may lead to reduced lateral stiffness, strength and ductility in such members when compared to slender walls (aspect ratio greater than 2) that exhibit flexure-controlled behaviour (Kolozviri, 2013).

In recent years, fibre-reinforced polymer (FRP) bars are proposed as a feasible alternative to steel as concrete reinforcement in areas where environmental conditions are adverse to steel reinforcement. Glass FRP bars (GFRP) are cheaper than carbon FRP bars (CFRP) and aramid FRP bars (AFRP) in North America. These bars have high strength-to-weight ratio, fatigue resistance, low thermal conductivity, and exhibit a linear-elastic behaviour up to failure (Vint, 2012). Mainly, GFRP bars do not rust or corrode, which remove the maintenance and rehabilitation costs caused by corrosion in conventional infrastructure construction (Vint, 2012).

Despite the lower elastic modulus of GFRP material than that of steel, studies focusing on application of GFRP bars in beams, columns and slabs, have shown that FRP-reinforced elements can be designed to have comparable ultimate strength and serviceability performance to conventional steel-reinforced members (Mohamed, 2013). However, studies on usage of FRP bars in shear walls are scarce up to date (Mohamed, 2013). Yamakawa and Fujisaki (1995) tested seven low-rise specimens (aspect ratio of 0.8) reinforced with CFRP (carbon FRP) grids. Although fracture of longitudinal CFRP grids was occurred during the tests, leading to low ductility and

energy dissipation capacity in the specimens, significant self-centering behaviour was observed due to the elastic response of CFRP material. To improve the ductility, the authors added partial steel to two CFRP-reinforced specimens. Despite exhibiting high strength and stable cyclic response, only a slight improvement was observed in the ductility of hybrid specimens due to lack of confining reinforcement. Mohamed et al. (2014b) tested three glass FRP (GFRP) reinforced shear walls different aspect ratios. The walls reinforced exclusively with GFRP bars exhibited superior strength, stable cyclic behaviour and significant self-centering, but very limited energy dissipation capacity due to the elastic response of the GFRP material when compared to the RC specimens.

Recent research in composite materials science shows that mechanical properties of conventional concrete can be improved by adding a dosage of randomly-distributed short fibres to the concrete, known as fibre-reinforced concrete (FRC). Although the properties of FRC are dependent on shape, dimensions, material, and amount of the fibres, typically fibre-reinforced concrete have better tensile strength, ductility, and durability than plain concrete due to crack bridging and pullout mechanism of fibres (Lee and Barr, 2004). Acceptable costs and high stiffness of steel fibres compared to polymeric and natural fibres have made them suitable for usage in nowadays construction. Despite the widespread application of steel fibre-reinforced concrete (SFRC) in pavements, slabs, tunneling and hydraulic structures, behaviour of SFRC shear walls have not been addressed appropriately in the literature (Athanasopoulou, 2010).

Majority of the research on SFRC shear walls were aiming at simplifying the steel layout and reducing rebar congestion. Carrillo et al. (2012) tested six concrete low-rise walls (aspect ratio of 1) made with steel fibre reinforced concrete (SFRC) under dynamic excitation using a shake table. The specimens had fibre volume fraction of 0.55-1.00%. The walls experienced a diagonal tension failure at collapse, but showed acceptable amount of energy dissipation and stable behaviour at the target drift ratios. Kang and Yun (2013) investigated the behaviour of a lightly-reinforced, non-ductile low-rise wall (aspect ratio of 0.55) with 1.5% volume fraction steel fibres under cyclic loading. Zhao and Dun (2014) presented a restoring force model for SFRC walls validated through testing of five SFRC walls with aspect ratio of 2. Response of the walls having similar steel reinforcement but different fibre ratios showed that fibres dosage has negligible effect on ultimate strength of the walls. Athanasopoulou and Parra-Montesinos (2013) investigated the behaviour of five low-rise shear walls (aspect ratio of 1.2 and 1.5) containing steel or polyethylene fibres under

cyclic loading, studying the possibility of relaxing the requirements for web and confinement reinforcement ratios. The fibre-reinforced walls exhibited a stable hysteresis response with drift capacities comparable to RC specimens, despite the complete elimination of confinement reinforcement in the boundary regions of the walls.

## **1.2 Research Objectives**

This study focuses on behaviour of low-rise walls which exhibit limited displacement capacity in comparison to slender walls. A hybrid scheme of FRP-steel vertical reinforcement is proposed for new construction of low-rise shear walls. The response of such walls are investigated experimentally and analytically to study the following objectives:

- Potential of the innovative system of hybrid FRP-steel reinforced shear walls to achieve comparable strength, stiffness and ductility with conventional RC walls under in-plane cyclic loading.
- Potential of elastic response of FRP material to enhance the self-centering capacity of shear walls.
- Addressing the most suitable arrangement of hybrid reinforcement in terms of design parameters such as maximum ductility and minimal residual displacements.
- Adequacy of the hybrid system for areas with seismic risks in terms of energy dissipation capacity, serviceability and residual displacements.
- Accuracy of the developed analytical model to be used for further design applications and development of design guidelines for the proposed innovative system.

Also, steel fibre-reinforced concrete (SFRC) is used in the hybrid specimen to discuss the following issues:

- Potential of fibres for reinforcement relaxation suggested in the literature.
- Potential of SFRC to increase damage tolerance in low-rise walls.
- An analysis model for SFRC shear walls.

Advantages and limitations of the proposed system are discussed.

## **1.3 Methodology**

The following steps are taken to address mentioned objectives.

In chapter 2, a preliminary finite-element (FE) analytical model, which is developed and validated based on the experimental results of steel- and GFRP-reinforced walls, is used to determine the most suitable hybrid scheme combining maximum ductility and minimum residual displacements. A conventional steel-reinforced wall, designed according to seismic considerations of CSA and ACI codes with the exception of the requirements for buckling prevention ties, is serving as a reference (control wall). However, the reinforcement buckling is not considered in the analysis. The FE model is used to investigate the effect of several hybrid reinforcement arrangements as an alternative for the control wall under cyclic loading. This parametric study provides the opportunity to investigate the effect of FRP bars size and location on important structural parameters such as the strength, energy dissipation capacity, ultimate displacement, self-centering and service ability limit state of the wall. Next, a simplified nonlinear seismic analysis is conducted to study the performance of hybrid system subjected to earthquake loading.

In chapter 3, details and results of the experimental program is presented. Two low-rise cantilevered specimens with aspect ratio of 1, the control wall and one of the hybrid GFRP-steel reinforced alternatives with fibre-reinforced concrete, are constructed and tested under quasi-static reversed cyclic loading. The relaxation in the buckling prevention ties allows for studying the SFRC effect on drift capacity of the walls. The response of each wall is monitored and recorded via proper instrumentation.

In chapter 4, the preliminary analysis model is modified to capture the test results with higher accuracy. The model is used to compare the response of the hybrid system with conventional steel-reinforced one in the case that buckling prevention ties are placed properly according to code provisions. Some other design aspects of hybrid FRP-steel reinforced walls and SFRC low-rise shear walls are addressed using the developed model.

Chapter 5 provides the overall research conclusions and recommendations for further work.

## **CHAPTER 2 ANALYTICAL MODEL FOR HYBRID FRP-STEEL REINFORCED SHEAR WALLS**

### **2.1 Introduction**

Fibre-reinforced polymer (FRP) bars are a feasible alternative to steel in reinforced concrete (RC) structures in areas where environmental conditions are adverse to steel reinforcement, since FRP-reinforced elements can be designed to have comparable ultimate strength and serviceability performance as conventional steel-reinforced members (CSA, 2012). Under cyclic loading, the load-displacement response backbone of FRP-reinforced members is approximately bilinear, with reduced energy dissipation and residual displacements in each cycle (Mohamed et al. 2014a; Tavassoli, 2013). Smaller residual displacements are desirable with the potential of reducing repair and rehabilitation costs after a seismic event. While research on concrete members reinforced with FRP bars has focused on beams, columns and slabs (Jakubovskis et al. 2014; Krall, 2014; Liu, 2011; Santos et al. 2013; Tobbi et al. 2012), studies on FRP-reinforced shear walls are scarce (Mohamed, 2013). Mohamed et al. (2014b) tested three shear walls completely reinforced with glass FRP (GFRP) bars under cyclic loading up to drift ratios of 3% in single curvature. The walls had three different aspect ratios. Although the energy dissipation capacity of the walls was low when compared to a companion RC specimen, it was found the GFRP walls exhibited satisfactory strength and resilience, with no strength degradation up to failure. These features would make GFRP walls suitable for use in areas with low seismicity, in which minimization of residual displacements allows for affordable repairs and immediate occupancy after the event (Mohamed et al. 2014a). Evidently, in areas in which the lateral demands are greater, this solution might be inadequate since the typical hysteretic response of a FRP-reinforced structure exhibits little ductility and limited energy dissipation. Therefore, as an alternative, the use of hybrid reinforcement consisting of steel and FRP rebars in shear wall structures is proposed. Steel lends ductility and energy dissipation to the wall, while the FRP material provides self-centering capacity. The performance of such a system would reduce post-earthquake maintenance and costs related to replacement or repair.

Since experimental data on this type of hybrid walls are unavailable, a robust analysis model verified with results obtained from FRP-reinforced and steel-reinforced concrete walls, would be

a useful tool to understand behaviour of the hybrid system, and make valuable design recommendations. In this study, such an analysis model for low-rise shear walls is developed using the finite-element (FE) method. First, an FE analysis model for walls reinforced entirely with either FRP or steel bars is developed and validated with experimental results. Next, a model for shear walls with hybrid FRP-steel reinforcement is proposed. The model is used to investigate important aspects of design, response and performance in several hybrid FRP-steel shear walls under in-plane loading. These aspects include optimal placement of bars, strength, energy dissipation, and self-centering behaviour. Both nonlinear static and dynamic analyses are used to analyze the walls. Finally, the advantages and limitations of the proposed hybrid FRP-steel reinforcing system are discussed.

## **2.2 Analysis Model for GFRP-Reinforced Shear Walls**

Finite-element program VecTor2 (Wong and Vecchio, 2002) is used to develop the analysis models for FRP- and FRP-steel reinforced shear walls. Developed for analysis of reinforced-concrete structures, program VecTor2 is based on the modified compression-field theory (MCFT), in which concrete is modeled as an orthotropic material with smeared, rotating cracks. The ability of program VecTor2 to predict the response of steel-reinforced shear walls has been shown in numerous research studies (Cortes-Puentes and Palermo, 2011; Cruz-Noguez et al. 2012; Gulec and Whittaker, 2009; Luu et al. 2013; Palermo and Vecchio, 2004, 2007; Sherstobitoff et al. 2012; Vecchio and McQuade, 2011).

In the analysis model, prepared by the third author of this study in a related project involving slender walls with GFRP bars, four-node quadrilateral elements was used to model the concrete, and the vertical reinforcing bars were modeled as truss elements. Horizontal reinforcement and stirrups at the boundaries were modeled as smeared reinforcement for simplicity, consistent with other studies (Cruz-Noguez et al. 2014a). It was assumed that the reinforcement and concrete were perfectly bonded, since this assumption was shown to provide satisfactory results (Palermo and Vecchio, 2007). GFRP was modeled as a brittle perfectly-elastic material. The pre-peak and post-peak response of concrete were modeled with a Hognestad parabola and a modified Kent-Park formulation, respectively. Concrete confinement provided by the closed stirrups at the wall boundaries was considered. The walls used to validate the program were the three GFRP-

reinforced walls tested by Mohamed et al. (2014b) (Fig. 2.1). These GFRP walls were all 3.5 m high, with a thickness of 0.2 m and widths of 1.5 m (specimen G15), 1.2 m (G12) and 1.0 m (G10). The mesh size was selected based on a sensitivity analysis, with smaller-sized elements at the bottom part to capture the higher nonlinear behaviour at the base of the cantilever walls (Fig. 2.2).

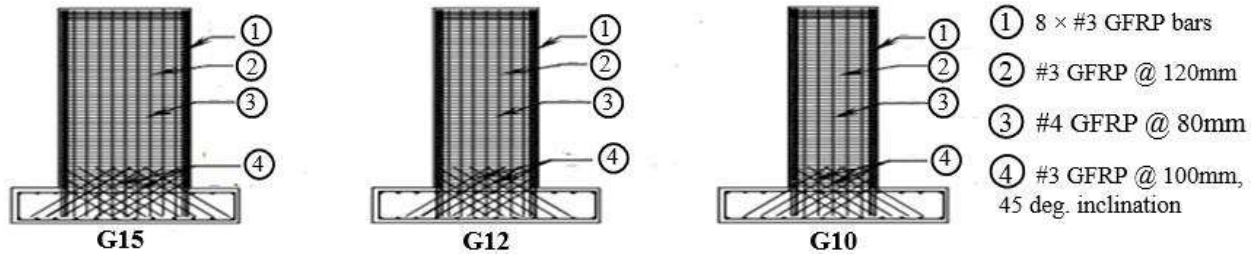


Fig. 2.1. GFRP-reinforced shear walls (mohamed, 2013)

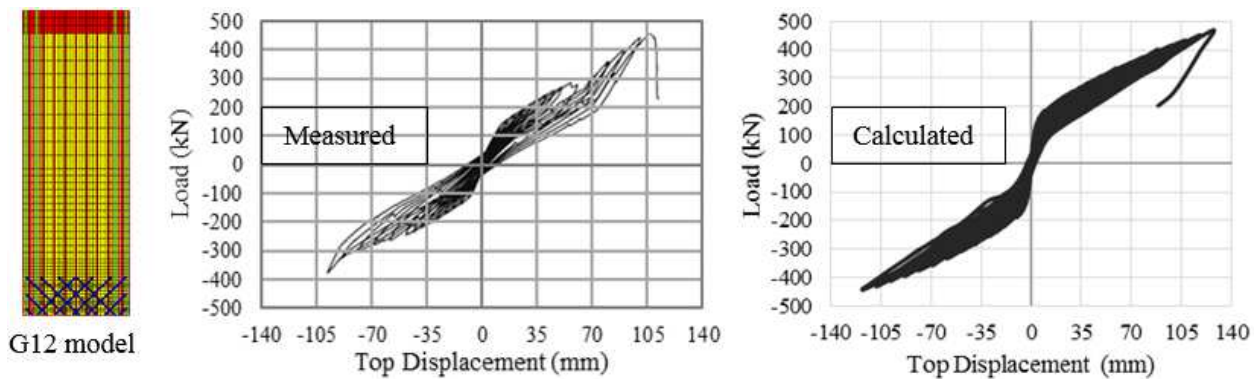


Fig. 2.2. Calculated vs. measured response for wall G12

As reported by Mohamed (2013), the concrete had a compressive strength of  $f'_c=40$  MPa on the test day. The sanded GFRP bars had an ultimate strength of 1412 MPa and a Young's modulus of 66900 MPa. Fig. 2.2 shows the model developed for wall G12. Due to space considerations, results for walls G10 and G15 are not presented, but they were found to be similar. It was observed that the developed model was able to predict the stiffness, strength and failure of the walls with reasonable accuracy.

### 2.3 Analysis Model for hybrid GFRP-Steel Reinforced Shear Walls

### **2.3.1 Design aspects**

Load-bearing shear walls are an effective system to provide strength and stiffness to structural systems. The height-to-length aspect ratio ( $h/t$ ) of the walls is an important factor, controlling the displacement capacity, mechanical behaviour, and failure mode of the wall. Low-rise or squat walls ( $h/t < 2$ ) are shear-dominated and tend to exhibit limited drift capacity in comparison to slender walls (Parra-Montesinos and Kim, 2004). Therefore, low-rise shear walls may be more vulnerable to seismic excitations that place larger displacement demands. Moderate intensity earthquakes can cause significant residual lateral displacements in steel-reinforced concrete shear walls, even those designed to current seismic codes (Erkmen and Schultz, 2009). To improve the seismic behaviour in low-rise shear walls, one alternative is a hybrid design that includes both steel and FRP rebars. The elastic behaviour of the FRP material is used to re-center the wall.

When designing FRP-steel hybrid members, several aspects must be considered. For instance, FRP materials have lower Young's modulus than steel, but typically have higher strength. Therefore, in terms of serviceability, to maintain the same stiffness and crack control found in conventional steel-reinforced concrete structures, a larger ratio of FRP reinforcement is required, when compared to the steel ratio in a conventional RC wall. Also, in terms of ultimate strength, the amount of FRP reinforcement required must be carefully chosen to avoid rupture of the FRP bars before concrete crushing. The vertical steel bars are placed at the boundary elements, in which the highest flexural strains are expected, taking advantage of the higher fracture strain of steel compared to FRP material. Yielding of the steel bars provides ductility to the system. The optimal place for the FRP bars is the middle of the wall, since this region experiences lowest flexural strains under cyclic loading caused by in-plane demands.

Shear design is assumed to be similar to that used in conventional RC structures under seismic loads, in which the shear strength is proportioned, so it is higher than the calculated flexural strength. In the proposed hybrid FRP-steel scheme, shear reinforcement is provided through steel rebars exclusively.

### **2.3.2 Wall models**

An experimental study conducted at the University of Alberta focuses on the seismic response of slender and low-rise hybrid GFRP-steel concrete shear walls. The size of low-rise specimens,  $1.8 \text{ m} \times 1.8 \text{ m} \times 0.15 \text{ m}$ , is determined by the capacity of available loading system. To allow for future

comparison of measured and calculated results, this study focuses on low-rise walls having the dimensions mentioned above. A FE model based on that presented in section 2.2 is used to investigate the effect of several reinforcement arrangements in low-rise walls (Fig. 2.3). The model represents a cantilever shear wall with concrete compressive strength of 50 MPa and 400 MPa steel reinforcement, designed to resist an in-plane bending moment of 1000 kN.m and a maximum shear associated to the flexural capacity of  $1000 \text{ kN} / 1.8 \text{ m} = 555 \text{ kN}$ .

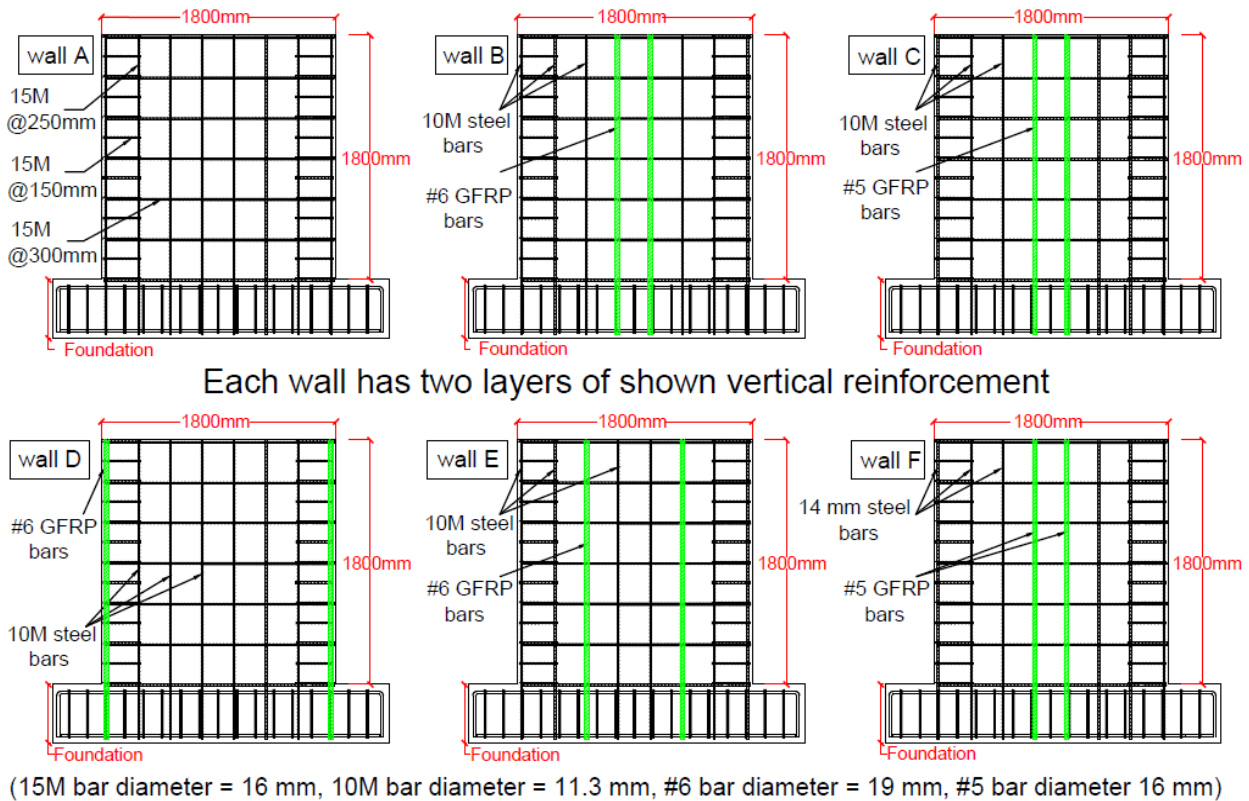


Fig. 2.3. Reinforcement detail of the models

The first model, wall A, is a conventional RC wall designed according to seismic considerations of CSA A23.3-14 code (CSA, 2014). The model has 8-15M (16 mm) 400 MPa steel bars as flexural reinforcement, and will serve as a control specimen (Fig. 2.3). 15M horizontal bars spaced at 300 mm are used as shear reinforcement in all the walls, providing a shear strength of 1372 kN based on the CSA A23.3-14 simplified method for shear design (CSA, 2014), greater than the shear demand associated to the attainment of the flexural capacity. The boundary reinforcement consists of 15M closed stirrups spaced at 150 mm.

To improve the self-centering capacity of this wall, while keeping a significant percentage of ductility and energy dissipation, a hybrid GFRP-steel reinforced alternative is considered. The properties of the GFRP bars used in the FE analysis are chosen based on commercially available products. An ultimate strength of 1200 MPa and Young's modulus of 60000 MPa are assumed for the GFRP material. Several design arrangements of GFRP and steel are explored to investigate the effects of bar position and GFRP bars size in the response. Wall B and wall C are designed to match the ultimate strength of wall A. For wall B, the four middle steel bars in wall A are replaced with 4 #6 (19 mm) GFRP bars, while the 15M steel bars at the ends are replaced with 10M (11.3 mm) steel bars as shown in Fig. 2.3. Wall C is a second design trial, which consisted of replacing the #6 GFRP bars of wall B with #5 (16 mm) GFRP bars. The purpose is to show the impact of different FRP reinforcement ratio on the calculated response. In terms of the influence that the placement of the GFRP bars have on wall self-centering, two additional models are created (walls D and E). These are hybrid walls in which the #6 GFRP bars are placed closer to the wall edges (Fig. 2.3).

The last model, wall F, is designed to show how serviceability requirements can be met with the hybrid design. Assuming maximum service stresses in the concrete and steel of  $0.4f_c$  and  $0.6f_y$ , respectively, a service lateral load of 360 kN is determined for wall A through a preliminary pushover analysis using the FE model. Since the Young's modulus of GFRP is lower than modulus of steel, meeting serviceability conditions in FRP-reinforced structures often requires a higher amount of reinforcement than that required to meet the ultimate limit state. This is more easily achieved by increasing the ratio of steel-to-GFRP. Wall F is designed by increasing the steel ratio. Wall F has #5 GFRP bars at the middle and 14mm steel bars as the steel reinforcement (Fig. 2.3). In contrast, wall B, designed to match only the ultimate strength of wall A, has 11.3 mm bars at the boundaries. Wall F is designed to have a similar stiffness with wall A at service conditions, and approximately the same ultimate strength of Wall B.

### **2.3.3 Results and discussion**

The models are subjected to cyclic loading as shown in Fig. 2.4. The calculated force-displacement hysteretic response for all walls is shown in Fig. 2.5. Table 2.1 shows a summary of significant structural parameters.

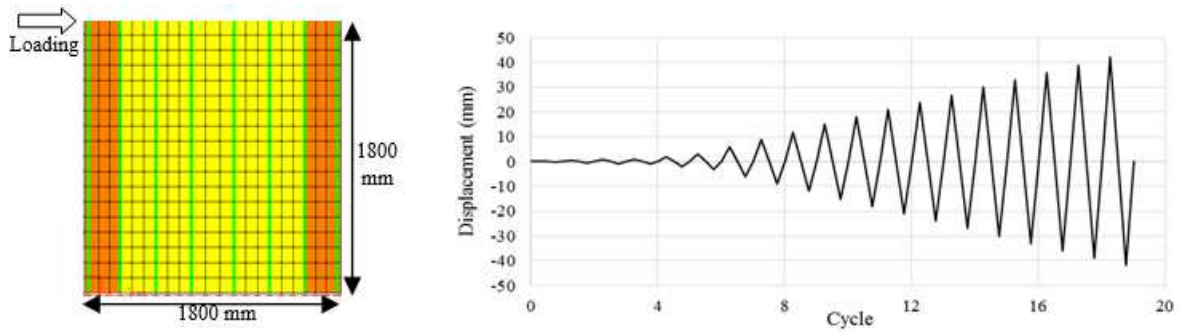


Fig. 2.4. Wall A model and loading protocol

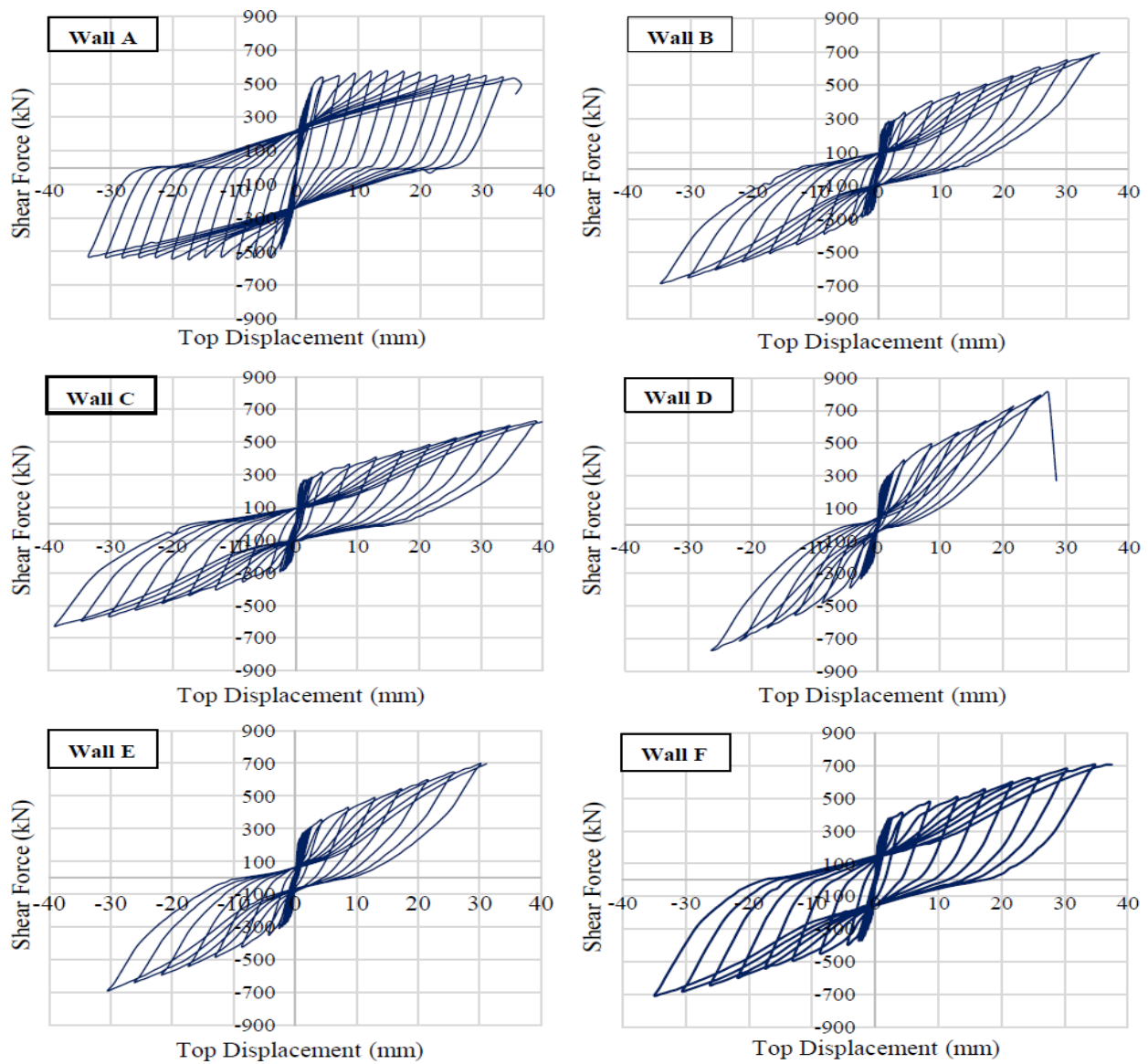


Fig. 2.5. Calculated base shear vs. top displacement responses

Table 2.1. Summary of analysis results for different models

<b>Model</b>	Calculated base shear (kN), section analysis	Calculated base shear (kN), FE analysis	Equivalent yield displacement (mm)	Ultimate displacement (mm)	Ductility	Self-centering ratio	Dissipated energy (area enclosed in last cycle) (kN.m)
<b>Wall A</b>	642	573	3	33	11	0.76	26.6
<b>Wall B</b>	635	684	2	34	17	0.38	15.8
<b>Wall C</b>	747	627	2	39	20	0.44	18.3
<b>Wall D</b>	870	794	2	26	13	0.15	5.7
<b>Wall E</b>	756	697	2	30	15	0.27	11.1
<b>Wall F</b>	734	706	3	37	12	0.50	22.6

### 2.3.3.1 Ultimate strength

The maximum calculated base shear of wall A is 573 kN, in agreement with the design objectives, while the average ultimate strength of the hybrid walls is 701 kN. Plane section analyses which included the effect of confinement at the boundaries, overestimates the base shears by approximately 12% for all the walls with the exception of wall B, in which the plane section analysis underestimates the ultimate strength by 7%. The difference is attributed to the fact that the walls are deep members in which Bernoulli beam theory does not hold. However, for preliminary analysis, the plane section analysis is shown to provide a reasonable estimate of flexural strength in low-rise shear walls.

### 2.3.3.2 Failure mode

Walls A, B, C and F fail by concrete crushing at the wall corners near the base, after significant yielding of the outer steel bars. Walls D and E, in which the GFRP bars are placed near or at the boundaries of the wall, fails due to rupture of the GFRP. This result is significant since it indicates that hybrid FRP-steel reinforced walls can be designed in a way that fracture of the GFRP bars does not occur before the confined concrete crushes, which is a desirable design target for elements that contain FRP reinforcement.

### 2.3.3.3 Displacement capacity

An attempt is made in this study to define ductility capacity levels in hybrid walls similar to those used in RC structures. An approximate bilinear trend is assumed for the envelope of hysteretic response, with an idealized yield displacement determining the change in the slope of the two branches. The yield displacement is determined with the equal-area method (energy absorption method) suggested by Park (1988). Since the envelope of the hysteretic response in hybrid walls is not associated with capacity deterioration, the slope of second branch was assumed to be average of the slope observed in post-yield part of the envelope, passing through ultimate point of the

response. This procedure is typically shown in Fig. 2.6. Table 1 shows the equivalent yield displacements obtained using this method and the resulting ductilities. Evidently, in hybrid walls with higher FRP-to-steel ratio, the change in slope will be controlled not by the steel yielding but the cracking of the concrete, as it occurs in FRP-reinforced members. In such cases, the definition of a yield displacement using the above technique would not be realistic. In general, all hybrid walls have higher ductilities than the RC wall. The walls with higher GFRP-to-steel reinforcement ratios (B and C), which do not meet serviceability requirements, have the highest ductilities, while the wall designed to meet both serviceability and ultimate strength limit state (F) has similar ductility with the RC wall (wall A).

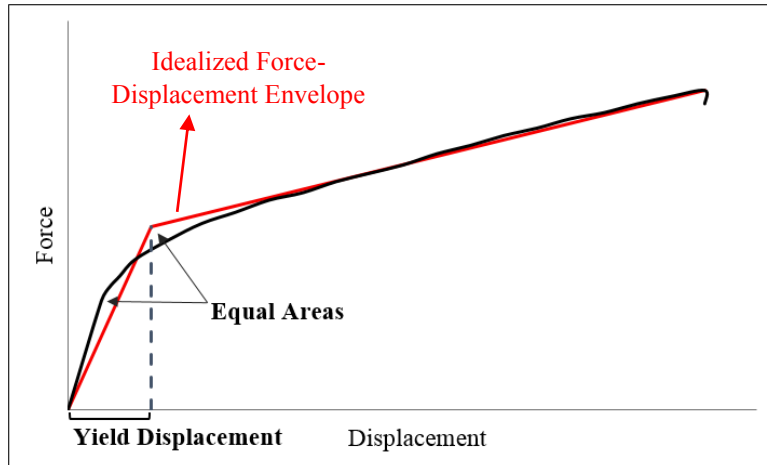


Fig. 2.6. Typical definition of idealized force-displacement envelope and yield displacement

#### 2.3.3.4 Self-centering

In terms of self-centering, when the top of wall A is pushed to its ultimate displacement capacity, 33 mm, a residual lateral displacement of 25 mm occurs. This significant residual displacement is typical of RC shear walls, even those designed to modern seismic guidelines (Cruz-Noguez et al. 2014b). To investigate the self-centering ability of the walls, the ratio of residual displacement to maximum displacement in the cycles is used. The self-centering ratio in the conventional steel-reinforced wall (wall A) is 0.76, while it is 0.38 and 0.44 for walls B and wall C, respectively. Wall C has a smaller self-centering ratio than wall B since it has a lower FRP reinforcement ratio. The analysis also shows that this ratio remains constant for a wall after yielding of the steel bars. For the last 5 cycles of each wall, the maximum difference in the calculated self-centering ratios

does not exceed 2%. A better self-centering ratio is achieved in walls D and E, as expected (0.15 and 0.27, respectively, compared to 0.38 in wall B). However, the mode of failure is rupture of the outer GFRP bars before concrete crushing. This results in a decreased drift capacity and energy dissipation capacity, as the ultimate drift decreases by 25% and 12% in wall D and wall E in comparison to wall B. The self-centering ratio in wall F is the highest of all hybrid walls (0.50), as it incorporates the highest steel-to-FRP ratio, but it is still lower than the RC wall self-centering ratio (0.76).

#### 2.3.3.5 Energy dissipation

In terms of energy dissipation, hybrid walls B and C have 64% of the energy dissipation capacity, in average, of wall A (Table 2.1). Walls D and E, with their premature failure due to GFRP fracture, have much smaller energy dissipation capacities. Wall F, designed to meet both serviceability and strength requirements, exhibits 85% of the energy dissipation shown by the RC wall. This is consistent with the findings by Mohamed et al. (2014b) in which the measured energy dissipation capacity of the GFRP-reinforced wall (G15) was about 60% of that measured in a hybrid wall reinforced with vertical steel bars and a grid of inclined GFRP bars with the height of 100 mm at the bottom (specimen ST15). If it is desired to increase the energy dissipated by the hybrid system in comparison to conventional RC, the amount of GFRP should be reduced, which in turn would decrease the self-centering capacity of the wall. Since having excessive residual displacements can result in structure collapse or high repair costs (Filiatrault et al. 2004), a balance between self-centering and energy dissipation is desirable. Nonlinear analysis presented in section 2.4 shows the seismic performance of hybrid systems.

#### 2.3.3.6 Serviceability

When subjected to this load, wall A experiences a top horizontal displacement of 1.5 mm (Fig. 2.5), but walls B and C experience top displacements of 6 mm and 9 mm respectively, likely exceeding serviceability requirements. Wall F exhibits 2 mm top displacement under the 360 kN service load. Response details can be found in Fig. 2.7 and Table 2.1. The backbone curves of the hysteretic response of wall A (steel-reinforced wall) and wall F (Fig. 2.7) show a characteristic tri-linear behaviour, in which the uncracked, cracked and yielded state of the walls can be readily identified. It is observed the uncracked (primary) and cracked (secondary) stiffness are very similar, while the slope of the third branch (tertiary) is considerably different. For wall A, the negative slope of the tertiary stiffness is associated with capacity deterioration, which is consistent

with the literature (Carrillo and Alcocer, 2012), while this slope is positive for the hybrid walls. The tertiary stiffness is always positive in hybrid GFRP-steel reinforced walls due to the nearly elastic behaviour of GFRP materials up to failure, and it is similar for walls with same amounts of GFRP (such as wall C and F). As a negative slope in the post-yield state may exacerbate stability problems (Rodgers and Mahin, 2011), hybrid systems have the potential to mitigate these unwanted effects.

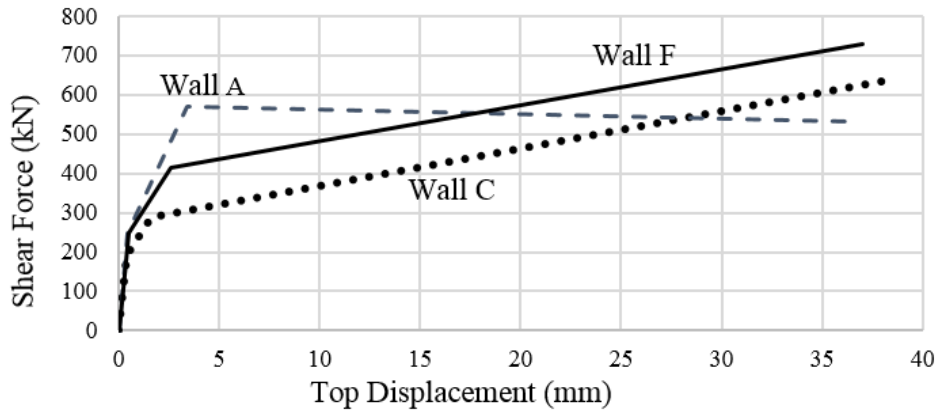


Fig. 2.7. Envelope of hysteretic response in wall A, C, and F

### 2.3.4 Seismic behaviour

A simplified dynamic analysis is presented to compare the behaviour of hybrid GFRP-steel reinforced walls C and F with the reference wall A under seismic loading. Wall F represents a hybrid wall compliant with service and ultimate limit states, while wall C does not meet serviceability conditions and it is expected to exhibit higher displacements. Four earthquake records are selected (Fig. 2.8). Assuming a 5% viscous damping value, the elastic response spectra of the chosen earthquakes are calculated and presented in Fig. 2.8.

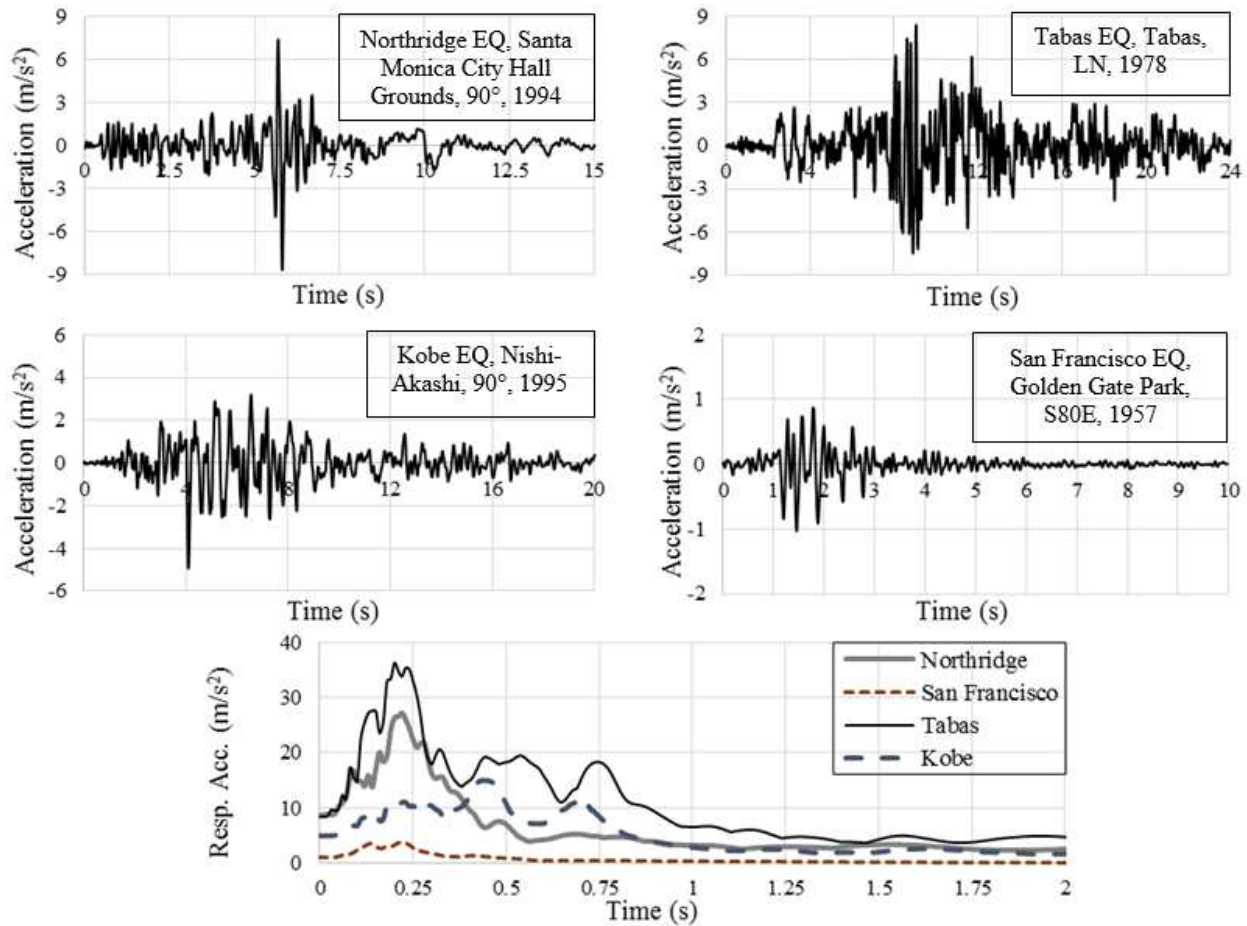


Fig. 2.8. Earthquake acceleration records (PEER, 2016), and calculated response spectral accelerations

A simplified nonlinear seismic analysis is conducted using the OpenSees FE platform (McKenna et al. 2000). It is assumed that the wall response can be represented as a single-degree-of-freedom (SDOF), mass-spring-damper system. The hysteretic response of the walls, calculated with program VecTor2, is represented using the “Hysteretic” material in OpenSees (Mazzoni et al. 2006). This tri-linear force-displacement model can be used to capture the lateral response of the walls. The unloading stiffness degradation parameters of the “Hysteretic” material in OpenSees are set to match the calculated VecTor2 response. It is noted that this simulation technique neglects important aspects of a rigorous dynamic analysis, such as the influence of the strain rate on the stress-strain response of concrete, steel and GFRP materials. However, Adorno-Bonilla et al. (2014) reported that this analysis can be used with satisfactory accuracy for design purposes. Fig. 2.9 shows the comparison between the hysteretic response of wall A calculated with VecTor2 and

the idealized response in OpenSees using the “Hysteretic” material. Due to space considerations, comparisons for the hybrid walls are not shown, but they are found to be similar.

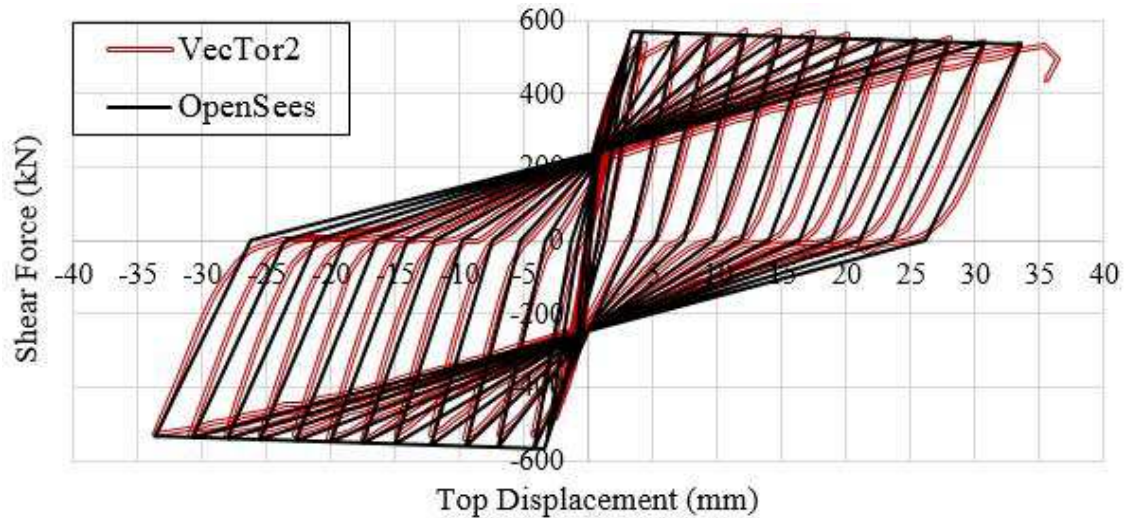


Fig. 2.9. Hysteretic model for wall A

Each wall is subjected to four earthquakes and each analysis is run for six different masses. The mass range is chosen so an ample period/frequency range can be investigated through the seismic excitations applied to the model.

Since the elastic stiffness of the walls can be obtained from the envelope of hysteretic responses in Fig. 2.5, considering an arbitrary mass range between  $75 \times 10^3$  kg and  $1700 \times 10^3$  kg results into a period range of 0.07 to 0.36 seconds. As a reference, the mass associated to a typical gravity load of  $0.08 A_g f'_c$  is equal to  $0.08 \times 150 \times 1800 \times 50 / 9.81 = 110 \times 10^3$  kg ( $T=0.09s$ ) for the walls in this study, which is a value close to lower end of the chosen range. The larger masses can be representative of multi-story structures with higher vibration periods. Investigating larger masses offers the opportunity to examine the response of the walls for the period range (0.07-0.40 seconds) in which the spectral responses of the selected earthquakes show the largest amplifications, as shown in Fig. 2.8.

The Newmark method with  $\beta=0.25$  and  $\gamma=0.5$ , and 5% initial stiffness proportional Rayleigh damping are used to conduct the analyses. Preliminary results show that the walls stay within the elastic range for the majority of the original input motions and masses considered. Since the nonlinear behaviour of the walls is the aspect of interest, a scale factor  $\lambda$  is applied to the

acceleration records to ensure that at least one of the walls would have a displacement demand of at least 75% of its calculated ultimate displacement. The same scale factor is used for the three walls for the same combination of earthquake and mass (Table 2.2). A summary of the maximum and residual displacements obtained for the walls is shown in Table 2.2 for all masses. Due to space considerations, only displacement and base shear histories for the mass of  $1700 \times 10^3$  kg for walls A, C and F are presented in Fig. 2.10.

Table 2.2 Results of seismic analysis

Earthquake		Maximum Displacement / Residual Displacement, (mm)					
Mass ( $\times 10^3$ kg)		75	400	725	1050	1375	1700
Northridge	$\lambda$	<b>1.0</b>	<b>0.5</b>	<b>0.31</b>	<b>0.32</b>	<b>0.23</b>	<b>0.18</b>
	Wall A	11/1	13/1	14/2	31/8	23/5	18/4
	Wall C	32/0	34/0	30/1	33/1	33/1	31/0
	Wall F	32/2	19/4	22/1	34/1	23/1	16/1
Tabas	$\lambda$	<b>0.7</b>	<b>0.2</b>	<b>0.2</b>	<b>0.15</b>	<b>0.15</b>	<b>0.13</b>
	Wall A	14/3	13/1	28/1	27/4	31/4	29/4
	Wall C	28/2	31/2	33/0	29/0	34/0	35/1
	Wall F	20/2	18/0	30/0	25/0	29/1	27/1
Kobe	$\lambda$	<b>1.3</b>	<b>0.45</b>	<b>0.45</b>	<b>0.41</b>	<b>0.34</b>	<b>0.34</b>
	Wall A	4/0	22/0	31/4	33/6	26/4	28/3
	Wall C	31/0	35/0	33/0	30/0	32/0	30/1
	Wall F	14/1	26/0	31/1	31/1	25/1	31/0
San Francisco	$\lambda$	<b>11.0</b>	<b>7.0</b>	<b>5.0</b>	<b>4.5</b>	<b>4.0</b>	<b>4.0</b>
	Wall A	24/1	28/10	26/7	33/10	25/5	27/5
	Wall C	36/1	30/0	31/0	29/0	31/0	33/1
	Wall F	32/2	30/1	26/1	27/1	24/0	31/0

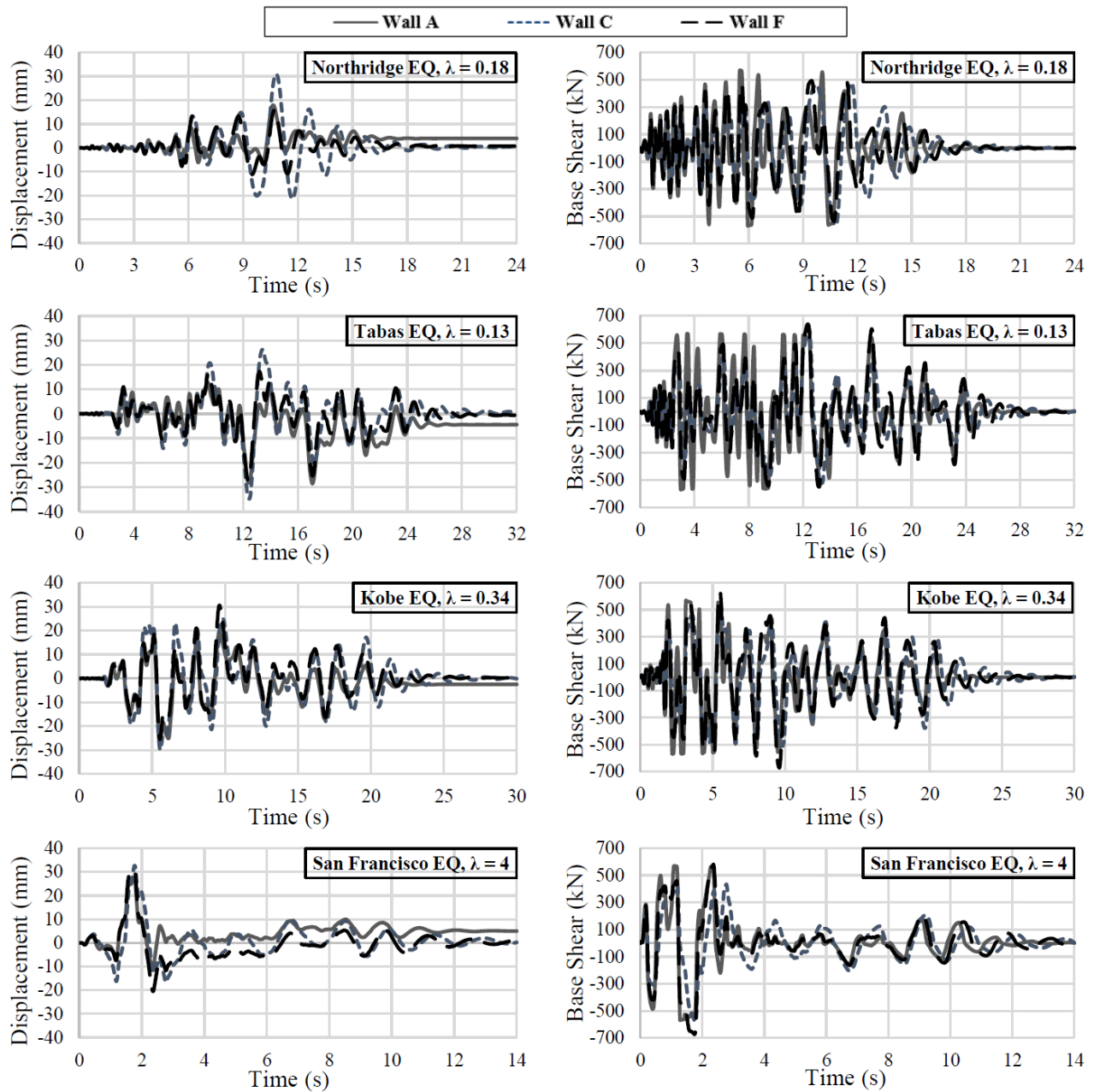


Fig. 2.10. Displacement and base shear histories for mass of  $1700 \times 10^3$  kg

In general, the results in Fig. 2.10 show that wall C exhibits higher displacements than the other walls for all earthquakes. Wall F has slightly higher displacements than wall A, but they remain comparable for a wide range of input motions and masses. While wall C is designed to meet the ultimate limit state but not serviceability requirements, wall F is designed to meet both. These results indicate that the displacements of the hybrid walls have a significant sensitivity to the initial

stiffness of the walls, and indicate that a rigorous dynamic analysis should be conducted to detect undesired response amplifications.

The base shears recorded in the three walls have a good correspondence in terms of waveforms, similar to the displacements, with maximum absolute values occurring approximately at the same time. This is encouraging, since it provides evidence that adequately designed hybrid walls can be incorporated into an existing building without major changes in the dynamic properties. Also, since the walls follow the same force-displacement hysteretic response calculated in the static cyclic analysis, walls C and F exhibit higher base shears than wall A.

The hybrid walls exhibit significantly less residual displacements than the RC wall. The analysis results show that wall A has a maximum residual displacement up to 10 mm (San Francisco earthquake), while it is 2 mm in hybrid wall F. Wall C, with the higher FRP-to-steel reinforcement ratio, exhibits the smallest residual displacements for all cases, but as discussed earlier it exhibits the highest displacements. This simplified analysis shows that hybrid walls can be designed using the same principles that control RC conventional construction in terms of site seismic hazard and frequency content consideration, in order to avoid undesirable amplification under seismic loading.

## **2.4 Conclusions**

This study is conducted to examine the benefits and limitations of an innovative system of hybrid FRP-steel reinforced, low-rise shear walls. An analysis model for GFRP-reinforced and hybrid GFRP-steel reinforced shear walls is developed and validated with experimental results. The model is used to design and investigate several configurations of hybrid GFRP-steel reinforcement in low-rise walls in terms of displacement, strength, residual displacements, energy dissipation, and seismic performance. Low-rise shear walls, due to their shear-dominated behaviour, usually exhibit low ductilities and may be vulnerable under seismic demands that place significant displacement demands.

In hybrid GFRP-steel low-rise walls, an arrangement of GFRP bars at the middle region of the wall together with steel bars at the wall boundaries is shown to achieve comparable strength and ductility with conventional RC walls under static cyclic loading. It also leads to a desirable mode of failure consist of crushing of concrete after substantial yielding of steel, with no rupture of GFRP bars. The hybrid system is shown to have significantly better self-centering behaviour than

its RC counterpart. Although the self-centering capacity in hybrid walls is expected to be less than that walls reinforced entirely with FRP, the energy dissipation capacity is better due to the presence of the steel.

The service limit state in hybrid walls can be met by adding more steel at the wall boundaries (wall F). This reduces the self-centering ability of the wall, since the plastic deformations of steel dominates the wall response. However, the energy dissipation increases, up to 85% of the reference RC wall. The additional steel at the boundaries increases the strength and decreases the displacement capacity of the wall. An important aspect to note is that a hybrid wall that has been designed to have similar initial stiffness with a RC wall, will have higher ultimate strength, since the backbone curve post-yield branch “shifts up”, while keeping the same slope. This translates into the need of well-designed adjoining elements and supports to carry the increased forces.

The seismic performance of an appropriately designed hybrid FRP-steel reinforced wall is comparable to RC members in terms of displacements. The initial stiffness of the walls is shown to have a major effect on the flexibility of the system. Simplified dynamic analyses show that the hybrid system is effective to minimize the residual displacements under strong ground motions.

The hybrid system can be considered as a promising alternative to conventional RC construction. However, a careful analysis needs to be conducted to determine if a given hybrid wall can meet the seismic demands with less energy dissipation capacity.

# CHAPTER 3 DAMAGE-RESISTANT REINFORCED CONCRETE LOW-RISE WALLS WITH HYBRID GFRP-STEEL REINFORCEMENT AND STEEL FIBRES

## 3.1 Introduction

In reinforced-concrete (RC) structures, shear walls are an effective system to provide strength and stiffness against lateral loads. RC walls should be designed to exhibit a ductile behaviour, so the structure can absorb and dissipate input energy of earthquakes (Hidalgo et al. 2002). This issue is more challenging in walls with low height-to-length ratios (aspect ratios), which tend to have a shear-dominated behaviour and limited drift capacity (Parra-Montesinos and Kim, 2004). Recent earthquakes have revealed that conventional steel-reinforced concrete (RC) shear walls can exhibit considerable damage and residual displacements even after moderate intensity earthquakes (Cruz-Noguez et al. 2014b; Palermo et al. 2005). These residual displacements can result in high post-earthquake repair costs (Filiatrault et al. 2004).

Recent advances in the science of composite materials have motivated the search for cost-efficient solutions to improve the behaviour of low-rise walls (walls with aspect ratios smaller than 2). Some studies have focused on usage of short steel fibres in shear walls, with the aim of simplifying the steel layout and reducing rebar congestion. Carrillo et al. (2012) tested six concrete low-rise walls (aspect ratio of 1) made with steel fibre reinforced concrete (SFRC) under dynamic excitation using a shake table. The specimens had fibre volume fraction of 0.55-1.00%. The walls experienced a diagonal tension failure at collapse, but showed acceptable amount of energy dissipation and stable behaviour at the target drift ratios. Kang and Yun (2013) investigated the behaviour of a lightly-reinforced, non-ductile low-rise wall (aspect ratio of 0.55) with 1.5% volume fraction steel fibres under cyclic loading. Zhao and Dun (2014) presented a restoring force model for SFRC walls validated through testing of five SFRC walls with aspect ratio of 2. Response of the walls having similar steel reinforcement but different fibre ratios showed that fibres dosage has negligible effect on ultimate strength of the walls. Athanasopoulou and Parra-Montesinos (2013) investigated the behaviour of five low-rise shear walls (aspect ratio of 1.2 and 1.5) containing steel or polyethylene fibres under cyclic loading, studying the possibility of relaxing the requirements for web and confinement reinforcement ratios. The fibre-reinforced

walls exhibited a stable hysteresis response with drift capacities comparable to RC specimens, despite the complete elimination of confinement reinforcement in the boundary regions of the walls. The authors suggested to evaluate this potential in walls with lower aspect ratios for further research (Athanasopoulou, 2010).

Fibre-reinforced polymer (FRP) bars are an attractive alternative for conventional steel reinforcement due to their high corrosion and fatigue resistance, high tensile strength, and light weight of FRP bars (Portnov et al. 2013). While a considerable number of studies have focused on application of FRP bars in beams, columns and slabs (Jakubovskis et al. 2014; Krall, 2014; Liu, 2011; Santos et al. 2013; Tobbi et al. 2012), few studies have investigated their use in shear walls. Yamakawa and Fujisaki (1995) tested seven low-rise specimens (aspect ratio of 0.8) reinforced with CFRP (carbon FRP) grids. Fracture of longitudinal CFRP grids was occurred during the tests, leading to low ductility and energy dissipation capacity in the specimens. However, significant self-centering behaviour was observed due to the elastic response of CFRP material. To improve the ductility, the authors added partial steel to two CFRP-reinforced specimens. Despite exhibiting high strength and stable cyclic response, only a slight improvement was observed in the ductility of hybrid specimens due to lack of confining reinforcement. Mohamed et al. (2014b) tested three glass FRP (GFRP) reinforced shear walls different aspect ratios. The walls reinforced exclusively with GFRP bars exhibited superior strength, stable cyclic behaviour and significant self-centering, but very limited energy dissipation capacity due to the elastic of the GFRP material when compared to the RC specimens. A finite-element (FE) model developed by Ghazizadeh et al. (2016) showed that the inclusion of steel reinforcement can be used to add energy dissipation and ductility to an FRP-reinforced concrete wall, and thus improve their seismic performance; however, experimental data on this type of hybrid walls are unavailable.

The literature shows that FRP bars have been used to eliminate the corrosion problem of steel, but to the knowledge of the authors, no study has targeted the enhancement of self-centering of a structural system as a design objective. This study presents an experimental program to investigate the response of two low-rise shear walls under cyclic loading, in which an attempt to mitigate the concrete damage and reduce residual displacements has been made. One of the specimens is a low-rise conventional RC wall, which will serve as a baseline for the comparison, and the other one is a hybrid FRP-steel reinforced concrete shear wall containing steel fibres, with similar geometry and reinforcement details as the control specimen. The RC wall was designed according to the

seismic considerations of the CSA A23.3-14 and ACI 318-14 codes (ACI 2014; CSA 2014), but neglecting the tie spacing required to prevent buckling. This design provides the opportunity to study SFRC effect on drift capacity of the walls experiencing the confinement relaxation suggested by Athanasopoulou and Parra-Montesinos (2013). The vertical hybrid reinforcement were designed using a finite-element analysis model developed for hybrid FRP-steel structures by Ghazizadeh et al. (2016) and the applicable provisions of Canadian code for FRP structures (CSA 2012). GFRP bars were placed at the middle region to improve self-centering behaviour, while conventional steel bars were placed in the rest of the web and the boundary regions. The objective was to observe if the hybrid scheme of reinforcement could achieve comparable strength, stiffness and ductility with conventional RC, while exhibiting less damage and residual displacements. The results of this study would be used toward development of more accurate analysis models and design recommendations for new construction of such innovative shear walls in areas with seismic risks.

## **3.2 Experimental Program**

An experimental study was conducted at the University of Alberta to address the seismic response of low-rise hybrid GFRP-steel reinforced shear walls. Two low-rise (squat) cantilevered specimens with aspect ratio of 1, a conventional RC wall and a hybrid GFRP-steel reinforced alternative with fibre-reinforced concrete, were designed and tested under static cyclic loading for this purpose.

### **3.2.1 Design and details of specimens**

Both walls had a rectangular cross section of 1800 mm long and 150 mm thick. They were 1800 mm in height, with a fixed connection to a stiff heavily-reinforced concrete block at the base. The RC specimen (control wall) was designed according to the seismic requirements of CSA A23.3-14 and ACI 318-1, with the exception of the requirements for buckling prevention ties. The buckling requirement was relaxed to investigate the ability of SFRC to prevent or delay buckling, as discussed later in this section.

Using both plane-section and FE analyses that accounted for the confinement effects of the concrete at the boundaries, the flexural reinforcement for this wall was designed to resist an in-plane ultimate bending moment of 1000 kN.m at the wall base. This value of moment resistance

was dictated by the available loading equipment at the I.F. Morrison Structures Laboratory at the University of Alberta. The actuator had a load capacity of 800 kN and a stroke length of 150 mm. 8-15M (16 mm) 400 MPa steel bars were placed as shown in Fig. 3.1, providing a vertical reinforcement ratio of 0.6%. The maximum base shear associated to the probable flexural capacity, accounting for overstrength in the materials, was calculated as  $1.47 \cdot 1000 \text{ kN.m} / \text{moment arm} = 817 \text{ kN}$ . The shear strength capacity was provided to avoid diagonal tension, diagonal compression, and sliding shear failure mechanisms. 15M horizontal bars with spacing of 300 mm (reinforcement ratio of 1.0%) were used as shear reinforcement as shown in Fig. 3.1, providing a shear strength of 1372 kN based on the CSA A23.3-14 simplified method for shear design, with diagonal compression strength limit of 4050 kN. The sliding shear strength calculated according to clause 11.5 of CSA A23.3-14 was 2052 kN. 15M closed stirrups spaced at 150 mm were used as the confining reinforcement in the boundary regions. Buckling prevention guidelines in the CSA A23.3 and ACI 318 codes require a spacing of 75 mm and 96 mm for the confining reinforcement of the control wall, respectively.

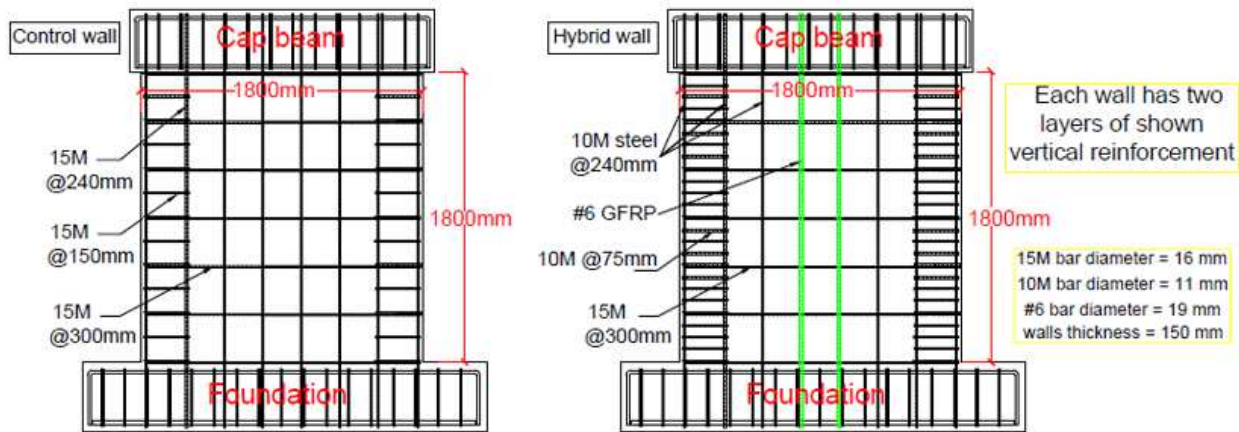


Fig. 3.1. Reinforcement details of specimens

To design the GFRP and steel reinforcements in the hybrid wall, the preliminary analysis model developed by the authors in an earlier study was used (Ghazizadeh et al. 2016) (the same model presented in chapter 2). It was determined that an arrangement of GFRP bars at the middle region of the wall would achieve comparable strength and ductility with conventional RC walls. Placing GFRP bars at the boundaries would place excessively high tensile strains in the GFRP bars, causing early rupture due to the low fracture strain of GFRP material (2% strain). Taking the

reinforcement of the control wall as a reference, the 4 middle steel bars were replaced with 4 #6 (19 mm) GFRP bars in the hybrid wall, while the 15M steel bars at the sides were replaced with 10M (11.3 mm) steel bars (Fig. 3.1). The size of the bars at the boundaries was reduced due to the fact that the GFRP material has a higher ultimate strength than the conventional steel. Since the ultimate flexural strength was comparable on the two walls, as calculated through the finite-element analysis, the same shear reinforcement was used in both walls, as shown in Fig. 3.1. The tie spacing at the boundaries of the hybrid wall was adjusted accounting for the smaller size of the 10M bars used at the region, to provide approximately the same buckling capacity using 10M closed stirrups and the same confinement to the concrete. Buckling prevention guidelines in the CSA A23.3 and ACI 318 codes require a spacing of 68 mm for the confining reinforcement of the hybrid wall.

### **3.2.2 Material properties**

60 MPa normal-weight concrete was ordered from the supplier for construction of both walls. The concrete in the hybrid wall was specified with 1.5% volume fraction of hooked-end steel fibres. Optimet® 9550 steel fibres with ultimate tensile strength of 1100 MPa, length of 50 mm, and aspect ratio of 55 (0.92 mm diameter) were used in the concrete mix for the hybrid wall.

The average concrete compressive strength of control wall was measured as 61 MPa based on the standard cylindrical tests performed at the test day on three cylinders. The three cylinders had strength of 59, 61 and 62 MPa. However, the mix provided for the hybrid wall by the concrete supplier had a compressive strength of only 40 MPa on the test day. The average stress-strain response of the cylinders are presented in Fig. 3.2. It is observed that the ultimate strain of plain concrete cylinders was about 0.43% while that of the fibre-reinforced cylinders was approximately 1.35%. Despite the difference in compressive strength, the same modulus of elasticity was observed in the cylinders. The average splitting tensile strength of the control wall and the hybrid wall were measured as 4 MPa and 3 MPa based on the standard cylindrical tests performed at the test day.

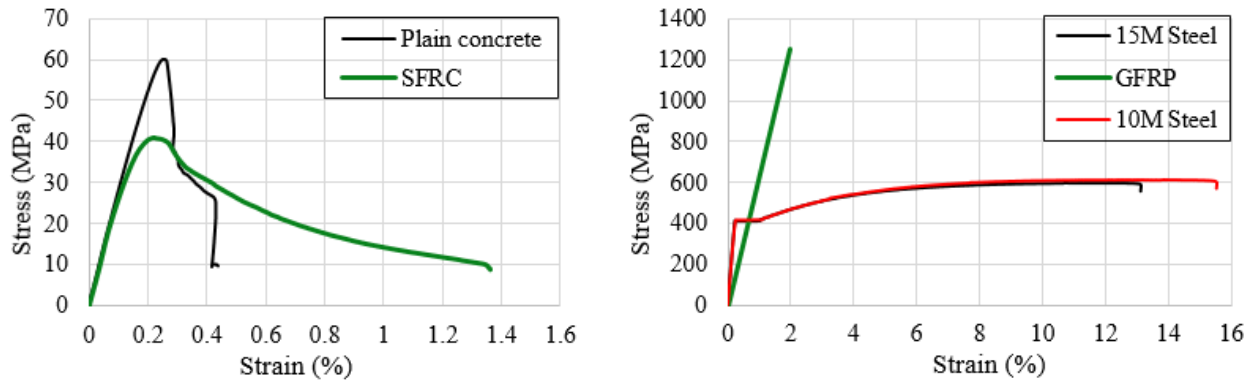


Fig. 3.2. Material properties

Steel-coupon tensile tests showed that both 10M and 15M steel bars had a yield strength of 414 MPa corresponding to yield strain of 0.22% as shown in Fig. 3.2 (Young’s modulus was 190 GPa). The sand-coated, high-modulus GFRP bars (TUF-BAR™) had linear elastic behaviour up to failure with ultimate stress and strain of 1254 MPa and 2.0% (Young’s modulus of 62.7 GPa).

### 3.2.3 Instrumentation, test setup, and loading protocol

Each specimen had two heavily-reinforced concrete blocks at the top and bottom. The foundation block at the bottom of the wall was anchored to the laboratory strong floor using 8 high-strength steel rods. The top block was used to place an out-of-plane restraint system and for loading purposes (Fig. 3.3). The walls were poured in horizontal position, then lifted using a frame as shown in Fig. 3.4 to avoid cold joints and streamline the construction process. The response of each wall was monitored and recorded via 38 strain gauges, 15 LVDTs (linear variable differential transformer), and 2 clinometers as shown in Fig. 3.5.

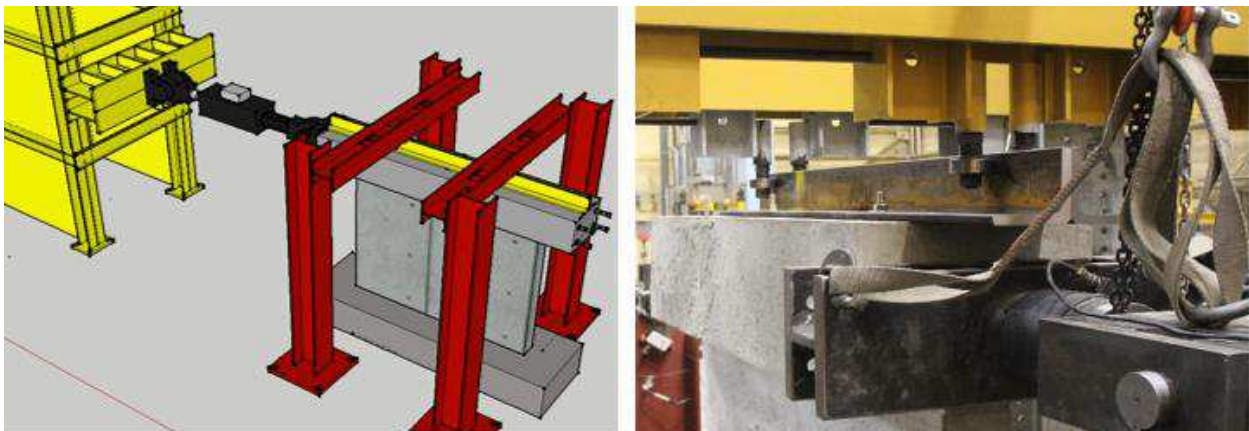


Fig. 3.3. Bracing frame



Fig. 3.4. Preparation and lifting

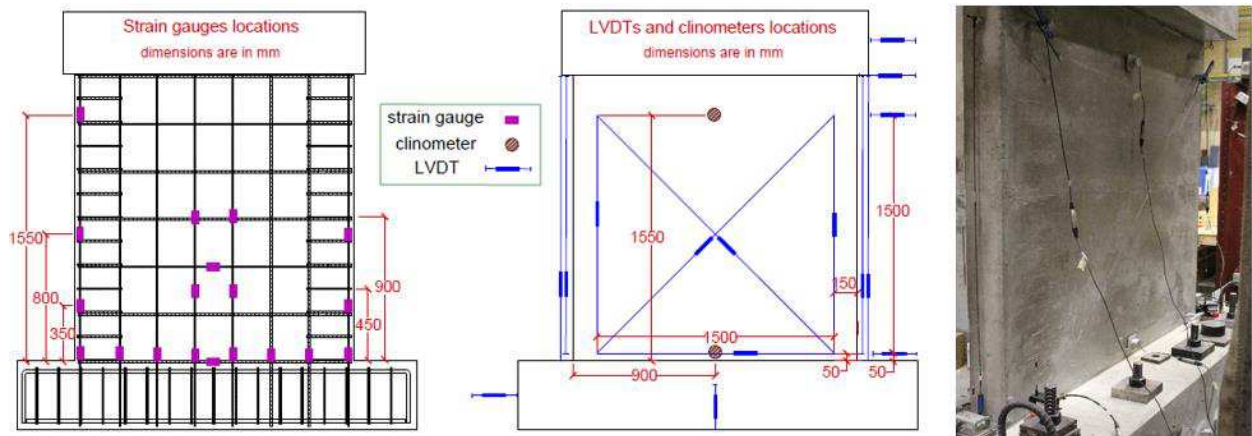


Fig. 3.5. Instrumentation

The walls were tested under in-plane, quasi-static reversed cyclic loading. Using a hydraulic actuator, lateral loads were applied to the RC block at the top of the specimens (Fig. 3.3 and Fig. 3.6). The tests were done in load-controlled cycles up to yielding of boundary bars, then continued in displacement-controlled cycles with the displacement history shown in Fig. 3.6. The load-controlled stage was divided into 3 different cycles based on the predicted yielding load presented in chapter 1. Every load cycle was repeated once to evaluate the stiffness and strength degradation. Previous research has shown that axial compressive loads would improve self-centering behaviour of the walls (Maciel et al. 2016). As it was desired to study the effects of self-centering provided exclusively by the GFRP bars, no gravity load was applied to the specimens. Evidently, if axial

load had been applied to the specimen, the observed ductility had been reduced due to the higher compressive strains in the wall toes. Therefore, the measured drift ratios constitute an upper range for the drift ratios to be found in concrete shear walls found in practice, and only valid if the wall system is very lightly loaded in the vertical direction.

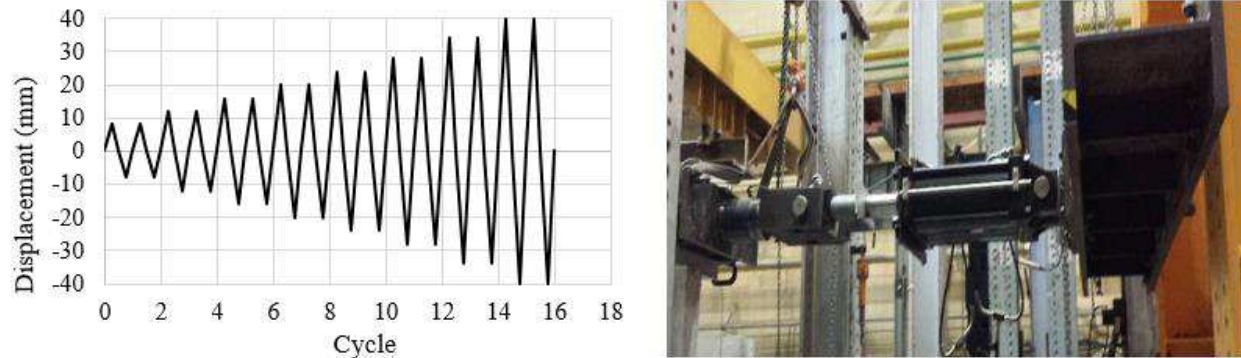


Fig. 3.6. Loading protocol and the hydraulic actuator

### 3.3 Experimental Results

Diagonal shear cracking, sliding shear and bond failure were not observed during the tests. The walls behaved in a ductile manner up to failure consisting of buckling of the bars at the boundary region. The following sections provide information on important design aspects and response of the walls.

#### 3.3.1 Hysteretic load-displacement response, strength, and stiffness

The lateral load versus top displacement response of the walls are presented in Fig. 3.7. Both walls experienced a stable hysteretic behaviour up to a top displacement of 40 mm. The hysteretic responses were reasonably symmetric in positive and negative directions. Defining the drift as the top of the wall lateral displacement divided by the initial height, both walls exhibited a drift capacity of 2.2% due to the same failure mode which will be discussed in next sections.

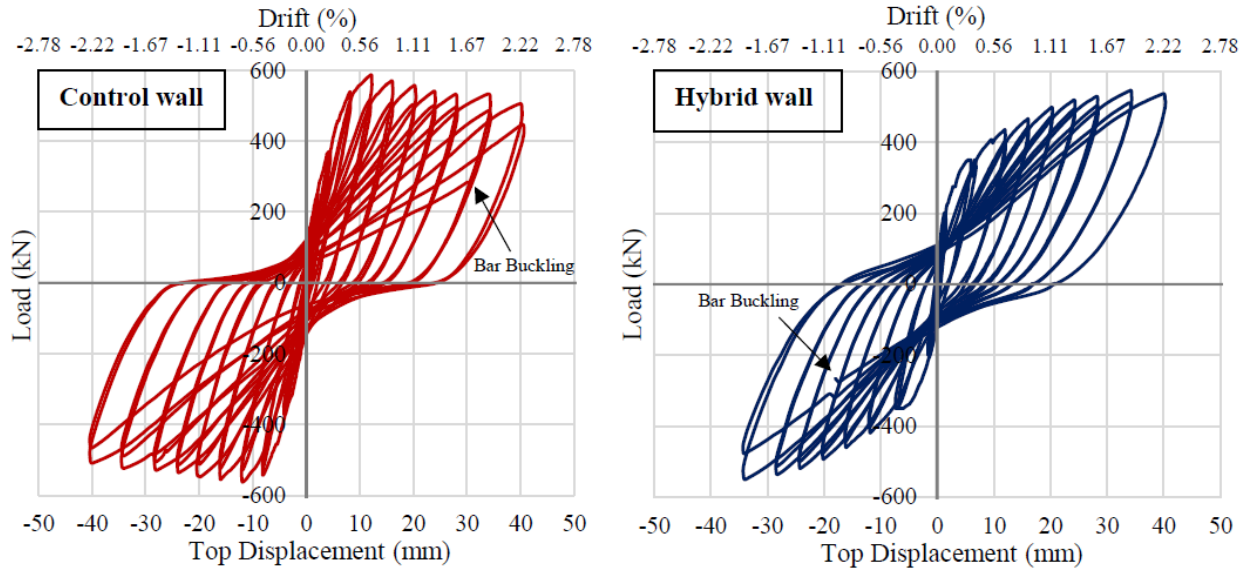


Fig. 3.7. Lateral load vs. top displacement response of the walls

The backbone curves of the hysteretic responses are presented in Fig. 3.8. It is observed that the backbone curves can be represented using a tri-linear model with uncracked, cracked and yielded (post-yield) states with reasonable accuracy (Carrillo and Alcocer, 2012). As one would expect, the initial stiffness of the walls (uncracked state) were very similar due the greater participation of the concrete compared to the reinforcing bars. The control wall had higher stiffness in the cracked state than the hybrid wall because once cracked, the reinforcement has a greater role in controlling the response. The Young's modulus of the GFRP material is lower than that of steel (by 68%). After yielding of the reinforcement, the response is strongly controlled by the reinforcement properties since the concrete in a large extent of the wall has cracked. While the response of the RC wall was governed by the flat plateau of the stress-strain response of the steel reinforcement and degradation of the concrete, in the hybrid wall the load-carrying capacity increased monotonically nearly up to failure. This was because of the quasi-elastic linear response of the GFRP material. The control wall underwent its peak lateral load at drift of 0.70%, and experienced strength deterioration in the post-yield state. The ultimate drift was associated with 15% capacity deterioration, while the hybrid wall did not experience strength deterioration. At drift of 1.1%, the control wall had 5% damage deterioration, while the hybrid wall had 90% of its peak load. The hybrid wall peak load was recorded at a drift of 2.0%. The monotonically increasing strength of the hybrid wall was desirable since the negative slope of post-yield state may exacerbate stability problems, as suggested by Rodgers and Mahin (2011).

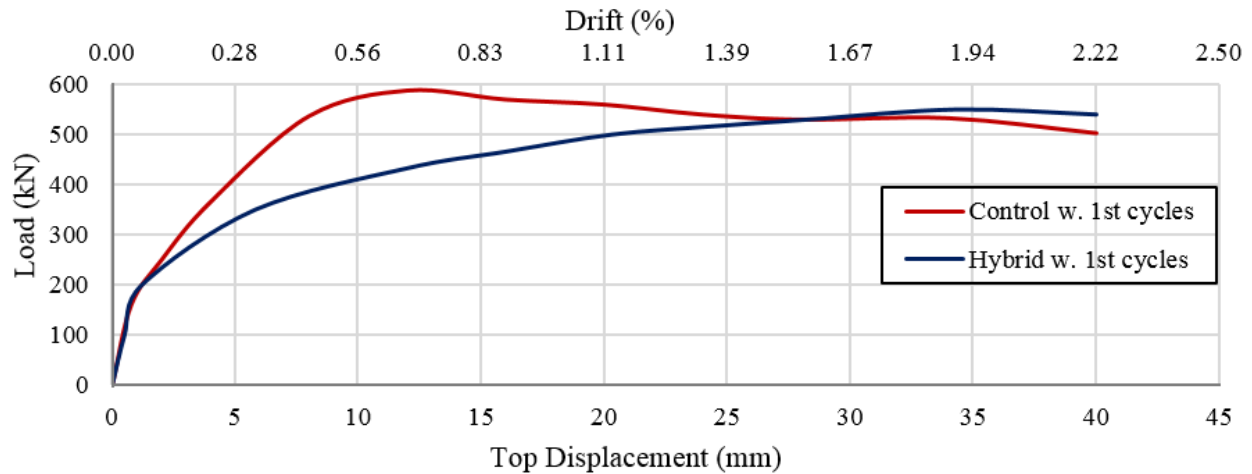


Fig. 3.8. Backbone curves of the hysteretic responses

The maximum measured lateral load was 588 kN in the control wall and 550 kN in the hybrid wall, satisfying the design target strength. Plane section analyses predicted 633 kN (a difference of 7.7%) for the control wall and 617 kN (a difference of 12%) for the hybrid wall. These analyses provided a reasonable estimate of flexural strength, considering the fact that Bernoulli beam theory of plane sections is not rigorously applicable in deep members such as low-rise shear walls. The correspondence of the measured response of the walls and the calculated response using the finite-element programs is discussed in a chapter 4.

To calculate stiffness retention capacity of the walls, peak-to-peak displacements of each hysteretic loop were used for calculation of the secant stiffness (Fig. 3.9) as suggested by Athanasopoulou (2010). Fig. 3.9 shows that the walls had very similar initial and post-yield stiffness (after 0.70% drift), but the control wall had higher stiffness in the cracked state since its bars yielded later than the hybrid wall boundary bars. Stiffness of the walls reduced significantly as the concrete cracked and boundary steel bars yielded. The ultimate secant stiffness was 7% of the initial stiffness.

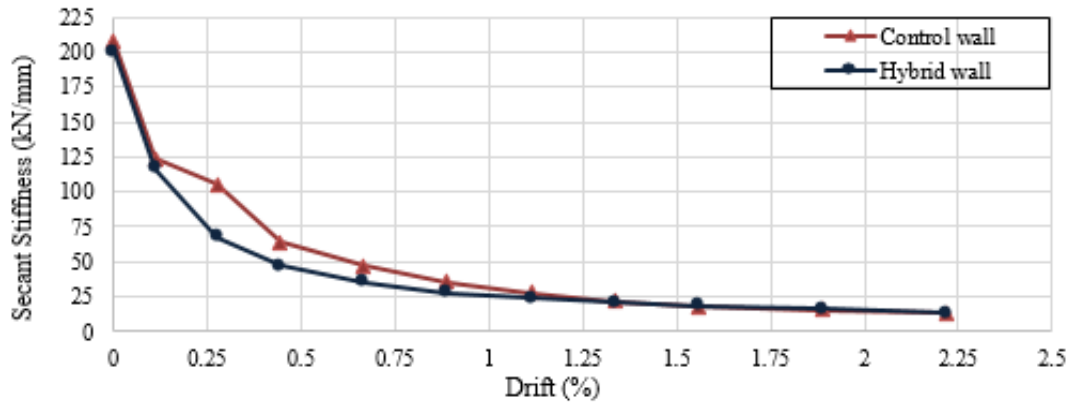


Fig. 3.9. Secant stiffness of the walls

### 3.3.2 Damage progression and failure mode

#### 3.3.2.1 First cracking

The first observed sign of cracking were two horizontal flexural cracks with width of 0.1-0.3 mm at each side of the walls near the toe region, under a lateral load of 210 kN in the control wall and 200 kN in the hybrid wall (during the second load-controlled cycle), at a drift of about 0.1% in both walls. This was consistent with the presented backbone curves (Fig. 3.8), in which there is a noticeable reduction in the initial stiffness of the wall after this displacement level. The response of the walls was nearly elastic up to this point. At this point, the maximum strain in the steel bars for the control wall was 0.15% observed at the base of outermost bars. In the hybrid wall, the maximum strain in the steel bars was 0.17% while the GFRP bars had a tensile strain of 0.08% at the base.

#### 3.3.2.2 Flexural-shear cracks

Three flexural-shear diagonal cracks and some more flexural cracks with the same width (0.1-0.3 mm) formed at mid-height of the control wall at a drift and load of 0.2% and 370 kN. Similar cracks formed in the hybrid wall at a drift and load of 0.3% and 350 kN. At this point, the tensile strains in the boundary steel bars of the control wall and the hybrid wall reached 0.24% and 1.1% respectively, while the GFRP bars had a strain of 0.24%.

#### 3.3.2.3 Reinforcement yielding

The outermost bars yielded at drift of 0.22% in the control wall, almost simultaneously with the appearance of the flexural-shear diagonal cracks. In the hybrid wall, the outermost bars yielded at drift of 0.17%, while the GFRP bars had strain of 0.15% at the base. All the steel bars were yielded by drift of 0.44%, while the control wall and the hybrid wall were experiencing 0.92% and 0.70%

of their peak load, respectively. The major cracks width were less than 1 mm at this drift in both walls.

#### 3.3.2.4 Post-cracking stage and major damages

As the tests went on, the cracks propagated and some new minor cracks formed as well. The crack pattern at three drift ratios for both walls are shown in Fig. 3.10. Major damage was concentrated at the lower part of the walls between the first and second stirrups, while cracks width of mid-level and top part of the walls did not pass 2 mm during the tests. Width of major cracks were 1 mm in the control wall and 1.5 mm in the hybrid wall at drift of 0.7% that the control wall experienced its peak lateral load. In both walls, flexural cracks of the sides reached to each other at the base at drift of 0.9%. Major cracks width increased up to 4 mm at 1.1% drift in the hybrid wall, while major cracks of the control wall had width of 3 mm at this drift. Spalling of concrete cover started at drift of 1.5% in the control wall. Up to this stage, both walls were experiencing almost a similar cracking pattern. This shows that usage of SFRC would not reduce the damage up to cover spalling. The maximum crack width was about 10 mm at the base of both walls at 1.5% drift. At higher drift levels, the concrete spalled in the control wall and exposed the vertical and horizontal reinforcements, while in the hybrid wall the concrete did not spall and the cracks retained approximately the same width. The ultimate state of the walls presented in Fig. 3.10 shows the effectiveness of SFRC to reduce the damage for drift ratios up to 2.2 %.

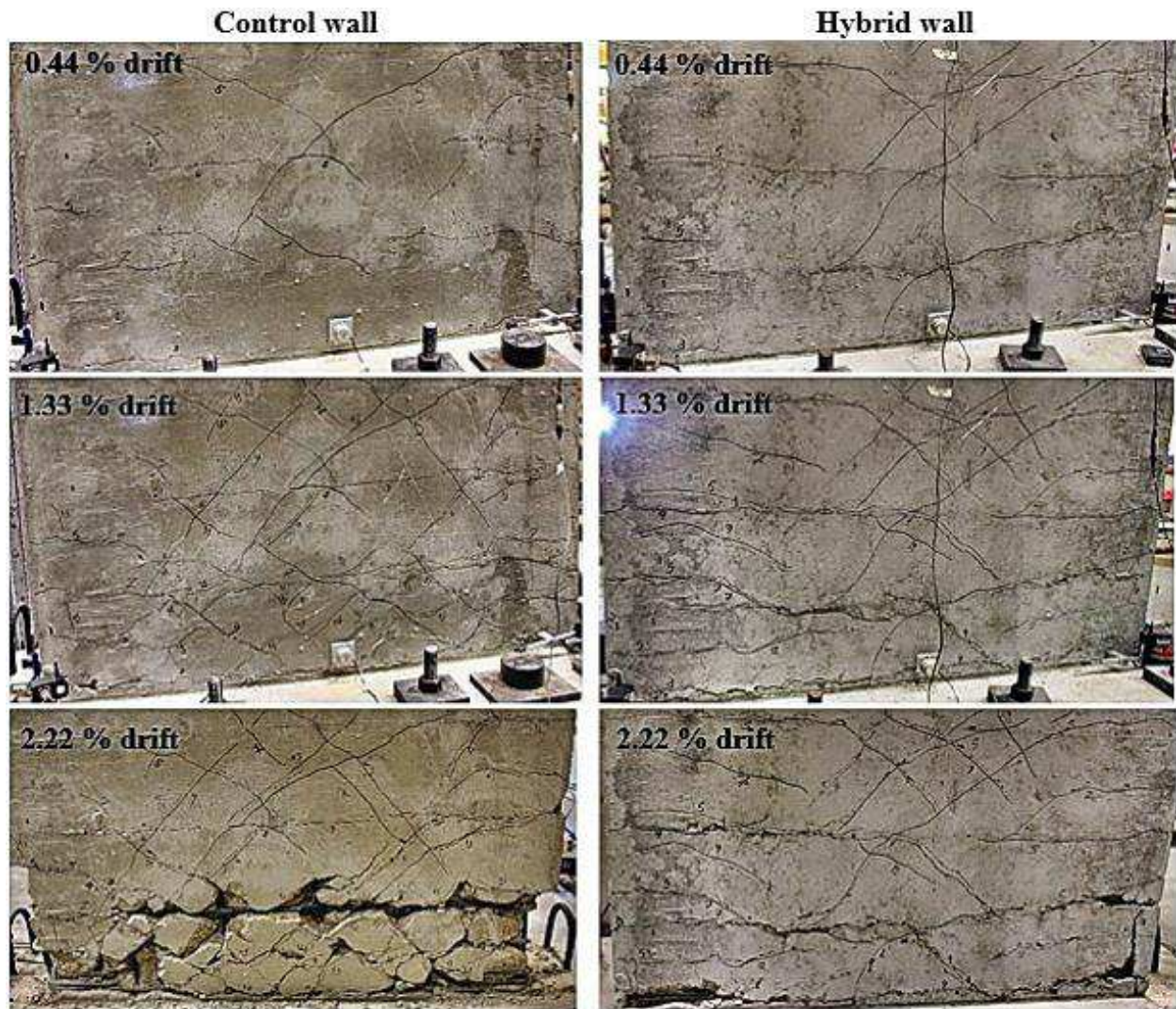


Fig. 3.10. Crack pattern and damage progression

### 3.3.2.5 Buckling of longitudinal bars

After reaching a top displacement of 40 mm displacement, (2.2% drift), the outer longitudinal bars in one side of the wall buckled when the wall was being reloaded. The buckling of the bars preceded the concrete crushing failure. The test was stopped due to the drop in strength of the wall in that cycle (22%). Measurements of the strain gauges on the affected bars showed that the bars had yielded at a top displacement of 4 mm and detached at a top displacement of 24 mm. In the hybrid wall, during the 40 mm displacement-cycle, the same buckling trend was observed. This shows that longitudinal bars buckling cannot be prevented by adding steel fibres, although some researchers suggested that presence of fibres can delay the bars buckling (Athanasopoulou and

Parra-Montesinos, 2013; Campione, 2011). In other words, hybrid wall achieved the same displacement capacity that it would have achieved in the case normal concrete had been used and the SFRC could not increase the drift capacity. Thus, by relaxing the confinement reinforcement, ductility of the wall and design safety would decrease. These results suggest that the relaxation of the tie spacing at the boundaries of shear walls when using SFRC is not feasible when buckling of the bars is critical. In the hybrid wall, some concrete cover at the plastic hinge region spalled off the wall when the bars buckled as shown in Fig. 3.11, but it was considerably less than the control wall. Despite the relaxation and bars buckling, the walls exhibited significant nonlinear behaviour.

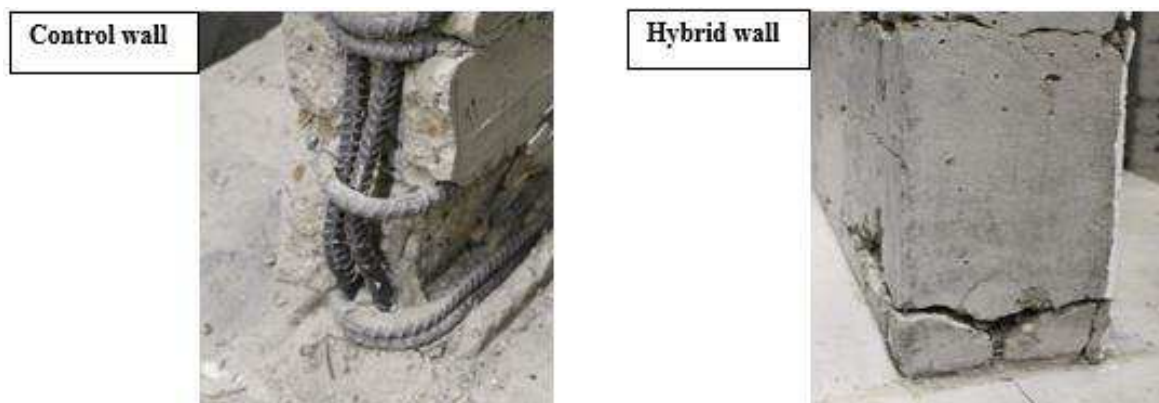


Fig. 3.11. Toe of the walls after bars buckling

### 3.3.3 Self-centering and energy dissipation capacity

Due to the elastic behaviour of GFRP bars, it was expected that the hybrid wall experience less residual displacements than the control wall. The residual displacement observed in each cycle is presented in Fig. 3.12 for both walls. For low drifts (about the yield point), the behaviour of the walls were very similar. In the post-yield state, the hybrid wall underwent less residual displacements. Ratio of residual displacement to maximum displacement was 0.63 in the last cycle of RC specimen, while this ratio was 0.50 in the hybrid wall.

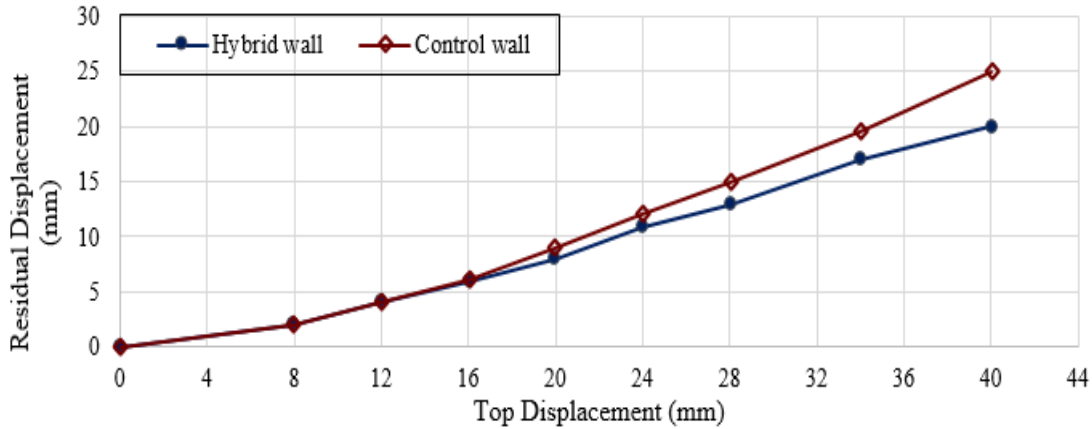


Fig. 3.12. Residual displacements of hysteretic cycles

Improved self-centering behaviour of FRP-reinforced walls would lead to narrower hysteretic loops and limited energy dissipation capacity (Mohamed et al., 2014b). Since input energy of earthquakes are expected to be dissipated in hysteretic cycles, a balance between self-centering and energy dissipation is desirable, which can be found in response of FRP-steel reinforced walls. Fig. 3.13 shows the area enclosed in each hysteretic cycle of the walls. Not only the hybrid wall had very close energy dissipation capacity to the control wall in different hysteretic loops, but also the area enclosed in the last cycle of hybrid wall (21.3 kN.m) was higher than the control wall (19.7 kN.m).

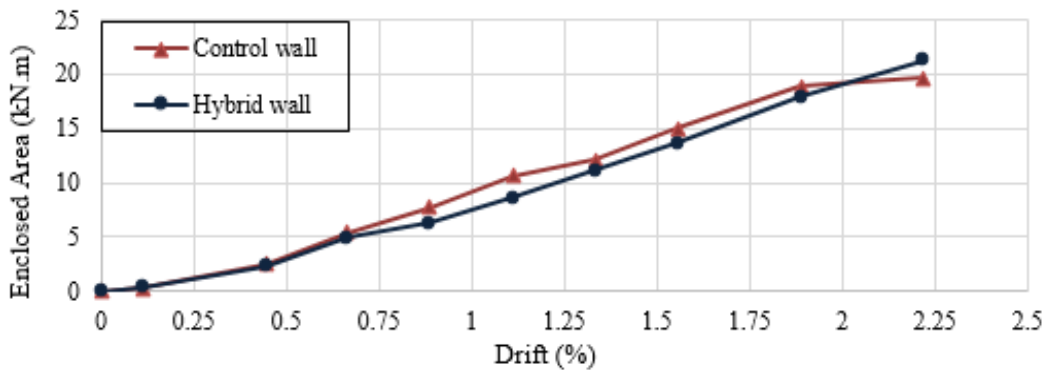


Fig. 3.13. Energy dissipation capacity through hysteretic cycles

### 3.3.4 Strains in longitudinal reinforcement

To provide further insight into the behaviour of the walls, the information collected from the strain gauges is discussed here. Fig. 3.14 shows the tensile strains at the base of outermost vertical

reinforcing bars on the same side of both walls. The vertical reinforcement in the hybrid wall yielded sooner (0.17% drift) than the vertical reinforcement in the control wall (0.22% drift) due to the lower steel reinforcement amount in the hybrid wall compared to the control wall. After yielding, the strains in the steel bars were higher due to the same reason. The strain gauges failed at drift of 1.33% in both walls.

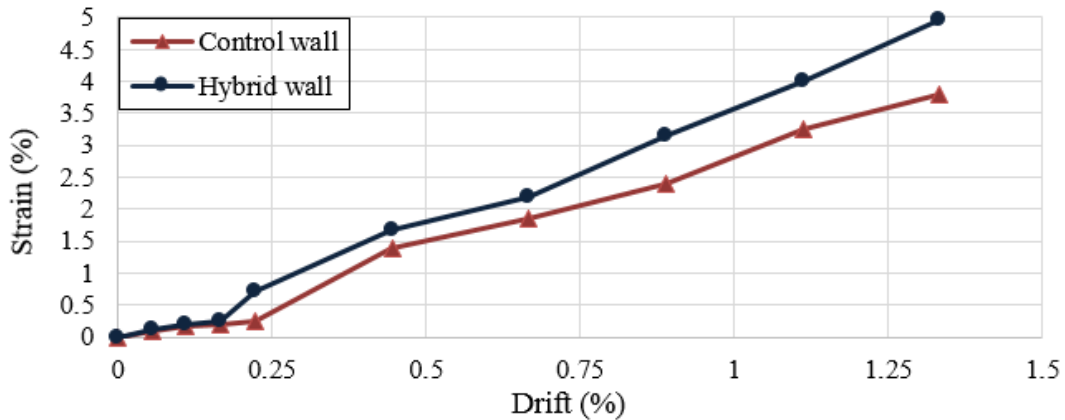


Fig. 3.14. Tensile strains of outermost reinforcement

Fig. 3.15 shows the strains at the base of GFRP bars. It is seen that the compressive strains experienced by these bars were negligible, and that the relationship between the tensile strains and drift ratio in the wall was approximately linear up to the failure point. At the ultimate displacement of the wall, GFRP bars experienced tensile strains up to 1.3%, which is 60% of their measured rupture strain. The maximum stress in GFRP bars shall not exceed the 25% of characteristic tensile strength under loads at serviceability limit state according to code requirements (CSA, 2012), which is by far satisfied.

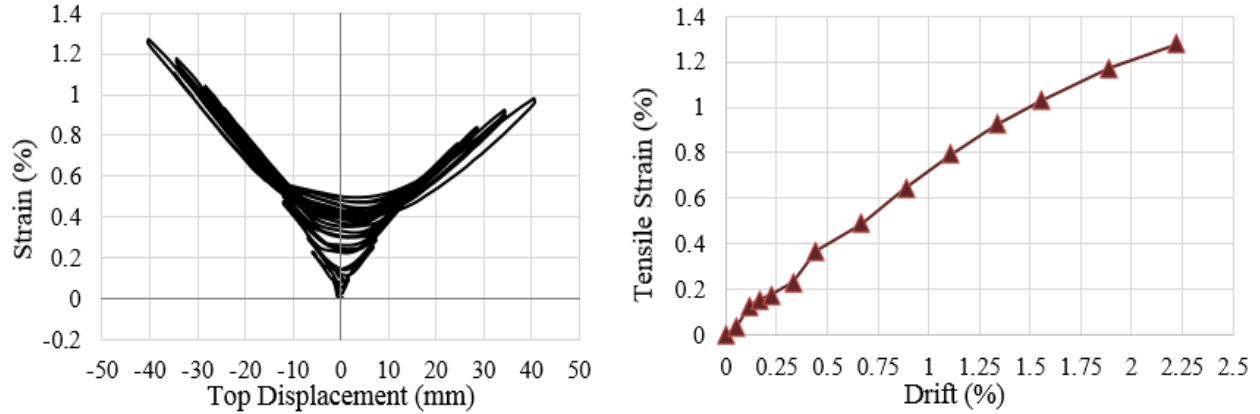


Fig. 3.15. Strains at the base of GFRP bars

For different cycles, the neutral axis (NA) depth was approximately calculated at the base level of the walls (Fig. 3.16) based on the available strain data collected from the strain gauges. As expected, prior to cracking the NA location was measured to be near the center of the wall. After cracking, the region in compression decreased rapidly and stabilized at about 10% of the wall width in average for both walls. Due to the strain hardening in the steel bars and the elastic response of the GFRP bars, the width of the block increased until the NA reaches about 14% in average at a drift ratio of 1.35%.

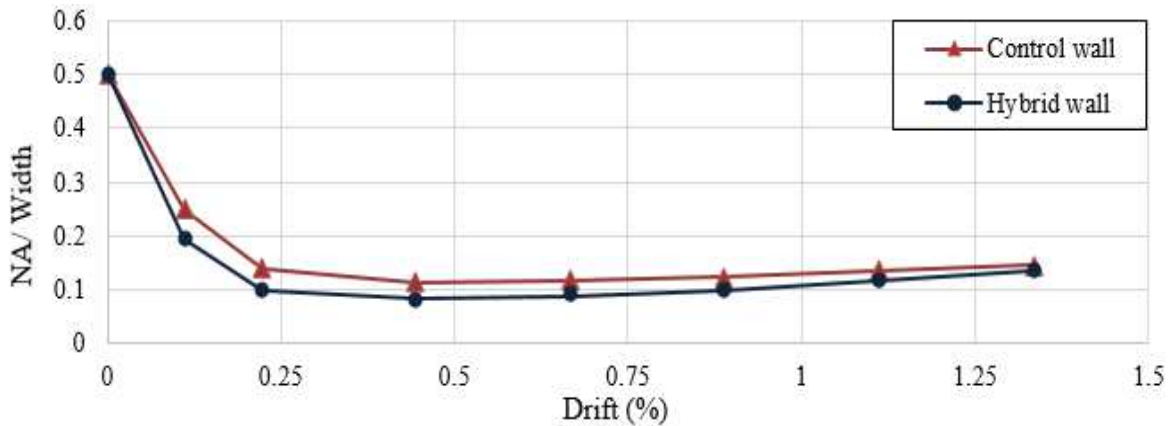


Fig. 3.16. Neutral axis depth

### 3.4 Conclusions

In this paper, behaviour of two low-rise shear walls is investigated experimentally under cyclic loading, a conventional steel-reinforced wall and a hybrid GFRP-steel reinforced alternative containing steel fibres. The following conclusions can be drawn from this investigation:

- The innovative system of hybrid FRP-steel reinforced shear walls is able to achieve comparable strength, stiffness and ductility with conventional RC walls under static cyclic loading with a proper design. By placing the FRP bars at the middle region of the wall, rupture of these bars at low drift ratios can be avoided and similar drift capacity to the steel-reinforced alternative can be achieved.
- The hybrid system is shown to have improved self-centering behaviour in comparison to its RC counterpart, while maintaining a significant energy dissipation capacity. Better self-centering behaviour can be obtained by increasing the amount of FRP reinforcement. This helps to avoid the excessive residual displacements that can result in high repair costs after earthquakes.
- The presented backbone curves show that response of hybrid FRP-steel reinforced walls are not associated with capacity deterioration. In order to shift up the cracked state part of backbone curve in the hybrid walls, more steel can be added to the wall boundaries, while the higher FRP ratio increases the post-yield state slope. This makes the hybrid walls suitable for a performance-based design.
- Usage of SFRC in shear walls increases the post-cracking damage tolerance and reduces pinching effect in the hysteretic response of the walls.
- Although the literature has suggested that usage of SFRC would increase the drift capacity and allow relaxation of confinement reinforcement in the walls, fibres are not able to delay buckling of longitudinal bars. Therefore, the proposed relaxation is not feasible in cases that buckling of boundary bars are critical.

Advantages and limitations of proposed system are discussed. Further research is needed to address other aspects and develop design guidelines for practical application.

# CHAPTER 4 NUMERICAL MODELING OF REINFORCED CONCRETE LOW-RISE WALLS WITH HYBRID GFRP-STEEL VERTICAL REINFORCEMENT AND STEEL FIBRES

## 4.1 Introduction

A large number of studies have focused on use of fibre-reinforced polymer (FRP) bars in reinforced-concrete (RC) members with the objective of reducing the corrosion issues associated with conventional steel reinforcement, but very few have focused on their usage in shear walls. Mohamed et al. (2014b) tested three glass-FRP (GFRP) reinforced slender walls under cyclic loading. The walls exhibited a stable hysteretic behaviour without strength degradation up to drift of 3%. Due to the fact that all the vertical reinforcement consisted of GFRP bars, the authors reported a quasi-linear force-displacement response up to failure, insignificant residual displacements up to 80% of the ultimate drift capacity, and very narrow hysteretic loops with negligible energy dissipation capacity. Although the absence of energy dissipation capacity is not desirable in seismic applications, the reduction of residual displacements is a desirable trait in seismic-resistant structures. Conventional reinforced-concrete shear walls designed according to the latest seismic specifications (ACI, 2014; CSA, 2014) exhibit large residual displacements even after moderate intensity earthquakes (Cruz-Noguez et al. 2014b; Palermo et al. 2005), which can result in high maintenance and repair costs (Filiatrault et al. 2004). To improve the energy dissipation capacity of FRP-reinforced walls, and promote ductility, the authors of current research suggested the usage of hybrid FRP-steel flexural reinforcement. In addition, damage can be reduced through the use of steel fibre-reinforced concrete (SFRC). Through an experimental program studying the behaviour of two low-rise shear walls conducted at the University of Alberta, it was shown that a hybrid steel-GFRP scheme of reinforcement in a low-rise shear wall made of SFRC could achieve comparable strength, stiffness and ductility when compared to conventional RC construction, while having improved self-centering behaviour.

Since the proposed innovative systems were shown to be a feasible alternative for RC construction, further research is needed to address other aspects and develop design guidelines for practical application. To reduce the time, costs, and efforts of conducting experimental programs for further

studies, valid numerical models can be developed based on the available tests data. With recent advances in finite-element (FE) methods, such models can be used to investigate the nonlinear behaviour of reinforced concrete structures for practical design and analysis applications (Palermo and Vecchio, 2007). Despite the extensive research conducted in this area, there are still some difficulties in predicting the cyclic response of low-rise shear walls (walls with low height-to-length ratio) with good accuracy due to the dominant shear behaviour in these members (Kolozviri et al. 2014b).

The majority of the models developed in the widely-used OpenSees platform (McKenna et al. 2000) are not able to consider shear-flexure interaction (Kolozviri et al. 2014a). A few researchers have tried to incorporate shear-flexure interaction into OpenSees fibre-based models based on the methodology proposed by Petrangeli et al. (1999). Massone et al. (2006) implemented a rotating-angle softened-truss model (Pang and Hsu, 1995) into a macroscopic fibre-based model for monotonic analysis of shear walls. The modeling results did not match the experimental results for the four low-rise walls due to the assumptions for coupling shear and flexure responses (Massone et al. 2006). Fischinger et al. (2012) added shear springs to a fibre-based macro model to account for aggregate interlock, dowel action and horizontal reinforcement resistance, and then simulated the response of a 5-story coupled wall tested on the shaking table under bi-axial excitation. This model was not validated against experimental data properly, and the modeling parameters were not studied in details (Kolozviri et al. 2014a). Recently, Kolozviri et al. (2014a-b) implemented the fixed-strut-angle model (Ulugtekin, 2010) into a fibre-based model to investigate cyclic response of shear walls with aspect ratios (height-to-length ratios) 1.5 to 2. Although predicting the response of these walls with good accuracy, this model underestimated the shear deformations for higher aspect ratios. Buckling and post-buckling behaviour of the bars were not considered in the model, and the used assumptions were not valid for walls with low aspect ratios (Kolozviri, 2013).

The FE program VecTor2 developed at the University of Toronto (Wong et al. 2013) is a versatile and power tool for analysis of reinforced-concrete structures assumed to be under plane stress conditions, such as shear walls. This program was developed based on the modified compression-field theory (Vecchio and Collins, 1986), in which concrete is modeled as an orthotropic material with smeared, rotating cracks. The ability of program VecTor2 to predict the response of slender shear walls (with aspect ratio greater than 2) has been shown in several studies (Cortes-Puentes

and Palermo, 2011; Cruz-Noguez et al. 2014a; Luu et al. 2013; Mohamed et al. 2014c; Palermo and Vecchio, 2007). A few studies have focused on simulation of low-rise walls (Gulec and Whittaker, 2009; Palermo and Vecchio, 2007), presenting a good estimation of load-displacement response. However, buckling and bond-slip effects were not considered in those models. The current research aims at presenting a robust model in VecTor2 for FRP-steel reinforced low-rise shear walls by simulating the response of the specimen with hybrid GFRP-steel reinforcement and steel fibre-reinforced concrete (SFRC) tested by the authors. The ability of the model to predict important aspects of the force-displacement response of the conventional wall and the innovative wall, and its limitations, are discussed. A parametric study is conducted to provide a better understanding of the innovative system

## **4.2 Summary of Experimental Program**

An experimental study was conducted at the University of Alberta by the authors to address the seismic response of low-rise hybrid GFRP-steel reinforced shear walls. Two low-rise (squat) cantilevered specimens with aspect ratio of 1, a conventional RC wall and a hybrid GFRP-steel reinforced alternative with fibre-reinforced concrete, were designed and tested under static cyclic loading (Fig. 4.1). The walls were designed according to the seismic considerations of the CSA A23.3-14 and ACI 318-14 codes (ACI 2014; CSA 2014), with some relaxation in spacing of the buckling prevention ties to study the potential of fibres for reinforcement relaxation suggested in the literature (Athanasopoulou and Parra-Montesinos, 2013). The control wall had normal-weight, 61 MPa concrete, with the average compressive stress-strain response shown in Fig. 4.2. The SFRC had compressive strength of 40 MPa with an ultimate strain close to 1.3% (Fig. 4.2). Steel coupons had a yield strength and young modulus of 414 MPa and 190 GPa, respectively. Sand-coated, high-modulus GFRP bars (62.7 GPa) with ultimate stress and strain of 1254 MPa and 2.0% were used in this study (Fig. 4.2). The walls were tested under in-plane, quasi-static reversed cyclic loading with no gravity load. Details of the experimental program and tests results are presented in a companion study (chapter 3).

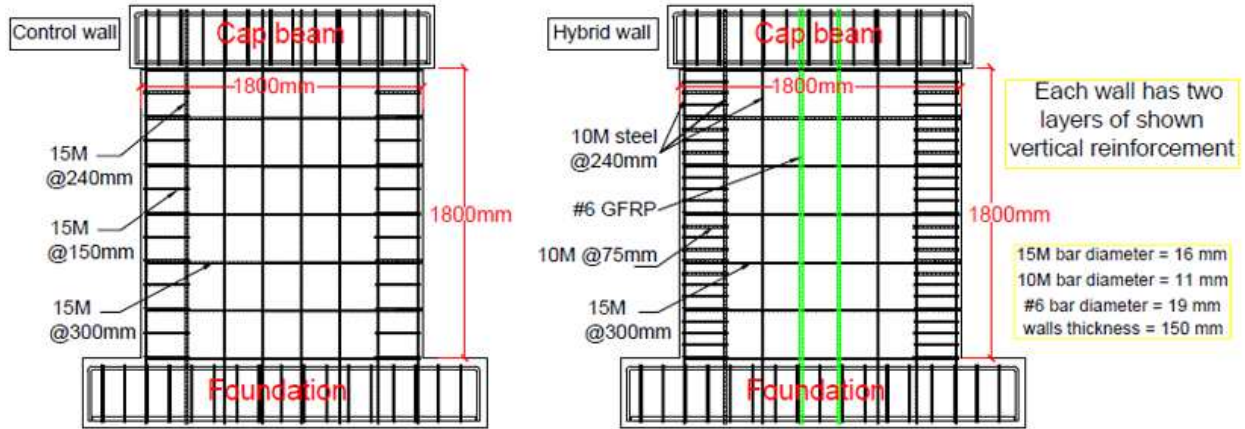


Fig. 4.1. Reinforcement details of specimens

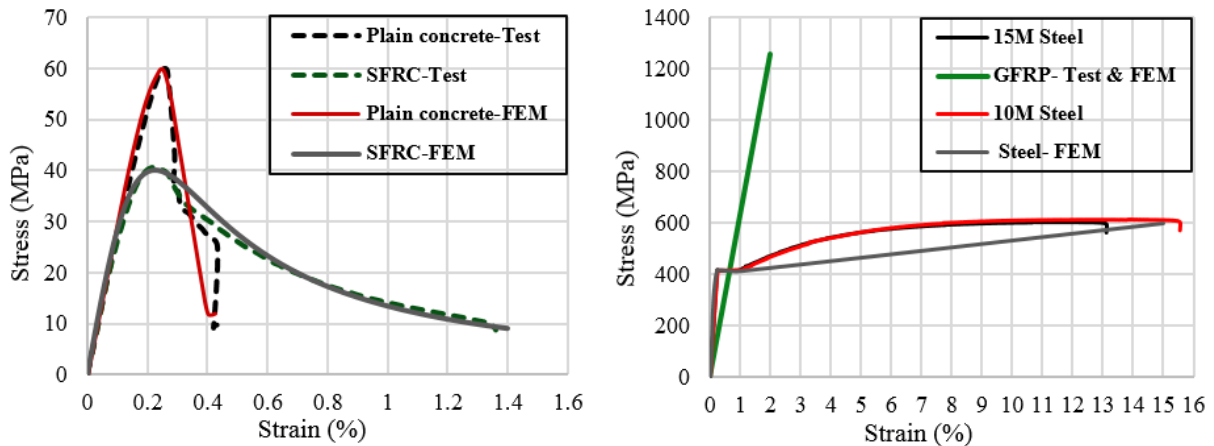


Fig. 4.2. Material properties in the tests and models

### 4.3 Analysis Model for Steel-Reinforced Concrete Walls

Four different analysis models of the steel-reinforced concrete wall (used as a reference, and termed “control wall”) were developed. The bond between steel and concrete, the hysteretic behaviour of the reinforcement, and the tension stiffening effect were the parameters that varied in each model, as discussed in the following section.

#### 4.3.1 Constitutive materials and model development

The models were developed based on the measured material and geometrical properties of the specimens. The program VecTor2 (version 3.8) contains a number of constitutive models for

concrete and reinforcement. In the analysis model for the control wall, the pre-peak and post-peak behaviour of the concrete in compression were modeled using Popovics (1973) high-strength model for concrete and the modified Park-Kent model (Scott et al. 1982), respectively (Fig. 4.2). The Palermo model (Palermo and Vecchio, 2002) was selected for the hysteretic response of the concrete to account for stiffness and strength degradation of the reloading branches. The strength of confined concrete was calculated using Kupfer-Richart model (Kupfer et al. 1969). Default parameters for compression softening, dilation and cracking in the concrete were used as suggested by Palermo and Vecchio (2007). Detailed information of mentioned models for concrete are available in the software manual (Wong et al. 2013).

The steel was defined using a tri-linear relationship as shown in Fig. 4.2. The shear reinforcement (stirrups) were modeled as uniformly-distributed (smeared) reinforcement within the concrete elements. This approach allows for a simpler and faster analysis compared to the alternative of using discrete truss elements for reinforcing bars, while maintaining sufficient accuracy (Cruz-Noguez et al. 2014a). The non-linear tension softening base curve proposed by Yamamoto (1999) was used in the analysis. Including tension softening in the analysis helps to determine the load-displacement response and ductility of the member more accurately (Wong et al. 2013). Despite the importance of tension stiffening effect in prediction of the accurate load-displacement response (Kharal, 2014), Luu et al. (2013) showed that this effect should not be considered in presence of dynamic loading. Hence, in one of the models developed in the current study (CW-M2) the tension stiffening effect was neglected to show the difference in predicted response. In three other models, the Kharal-Sheikh model for tension stiffening (Kharal, 2014) developed recently for steel- and GFRP-reinforced concrete was used. The flexural reinforcement (vertical bars) were modeled using truss elements. The bond-slip mechanism between the concrete and boundary steel reinforcement was defined using Gan-Vecchio stress-slip relationship (Wong et al. 2013), except in model CW-M1, in which the reinforcements were perfectly bonded to concrete to investigate the bond-slip influence in response of the model. The elastic-plastic Tassios model was assumed for dowel action of reinforcement. Two alternatives were considered for the hysteretic response of the reinforcement: In model CW-M4, Seckin (1981) model which includes Bauschinger effect was used as suggested in the literature (Gulec and Whittaker, 2009; Maciel et al. 2016; Mohamed et al. 2014c, Palermo and Vecchio, 2007). In other wall models, the Akkaya model in which the Seckin hysteretic model was modified to include the buckling effects (Wong et al. 2013), was used.

Response of these four models and effect of selected parameters are presented in the following section. Four-node, 120 mm × 120 mm rectangular elements were used to develop the model as shown in Fig. 4.3. A pushover analysis was conducted on one of wall models with three different element sizes as shown in Fig. 4.4 to study the sensitivity of the model to the selected mesh size. The models were subjected to static, lateral cyclic loading with the same displacement history applied to the test specimens as shown in Fig. 4.3.

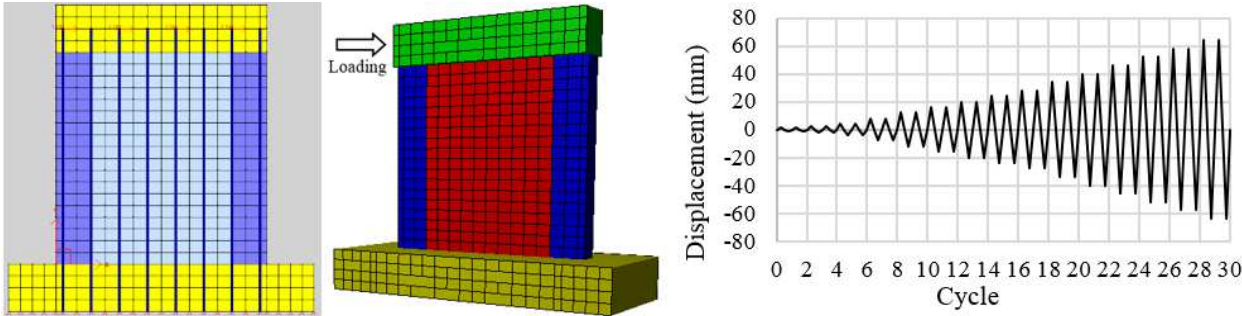


Fig. 4.3. Loading protocol and one of the models

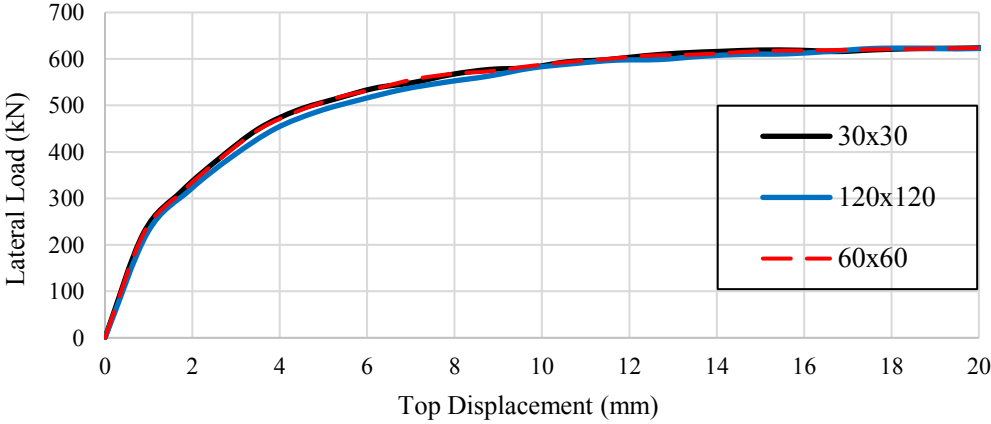


Fig. 4.4. Mesh sensitivity analysis results

**4.3.2 Model validation**

The calculated force-displacement hysteretic response of the models are presented in Fig. 4.5 and Table 4.1. All of models exhibited concrete crushing at the compressive corner at their ultimate displacement after yielding of the steel reinforcement as shown in Fig. 4.6.

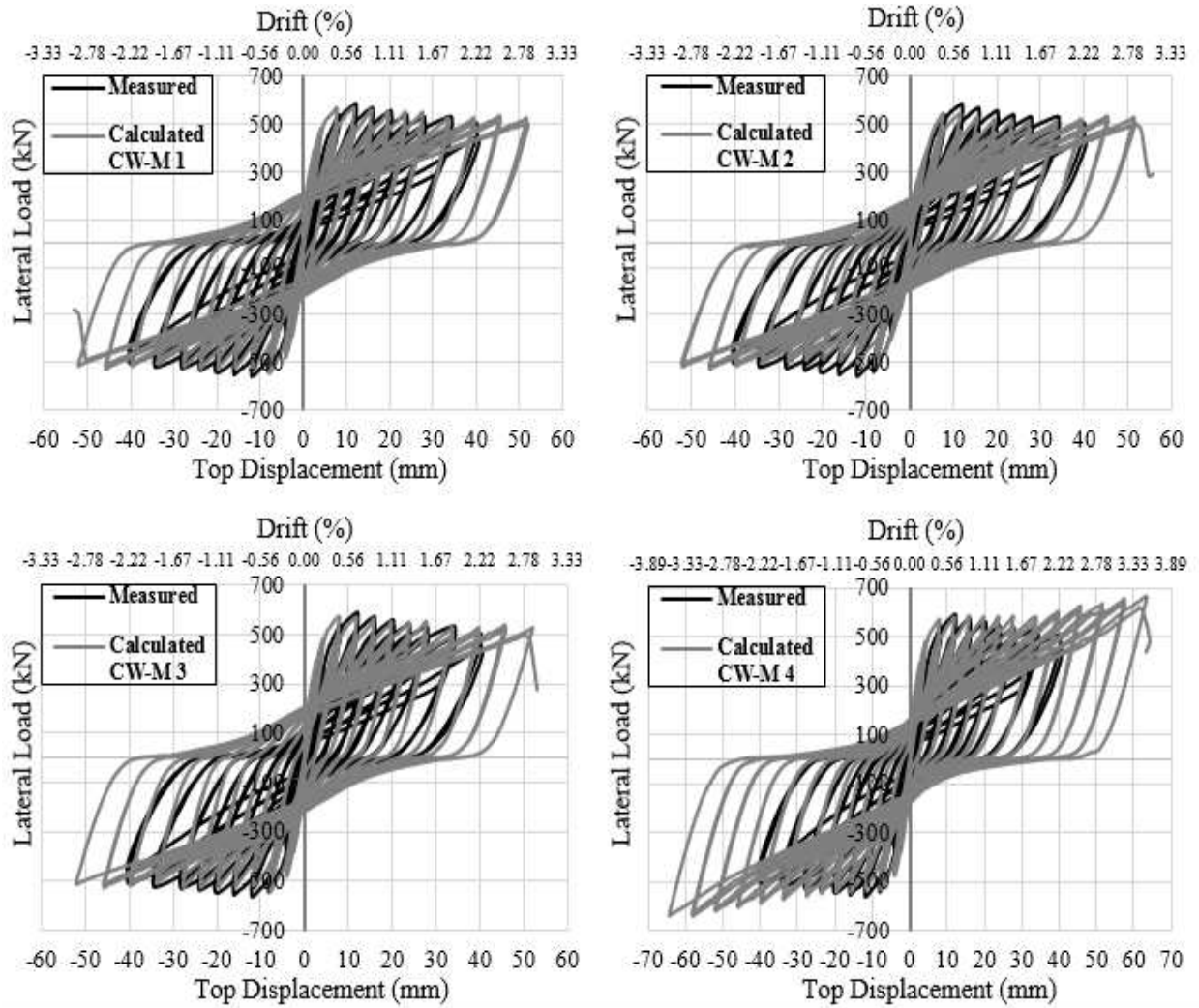


Fig. 4.5. Force-displacement response of the control wall models

Table 4.1. Summary of modeling results for the control wall

Models	Reinforcement hysteretic model	Bond model	Tension stiffening model	Peak load (kN)	Ultimate displacement (mm)	Peak load displacement (mm)	Initial stiffness (kN/mm)	Strength deterioration (%)
CW-M1	Akkaya	Perfect bond	Kharal-Sheikh	566	52	8-12	237	8
CW-M2	Akkaya	Gan-Vecchio	No stiffening	541	52	8-12	188	3
CW-M3	Akkaya	Gan-Vecchio	Kharal-Sheikh	567	52	8-12	237	8
CW-M4	Seckin	Gan-Vecchio	Kharal-Sheikh	660	64	64	237	----
<b>Test</b>				588	40	12	207	16

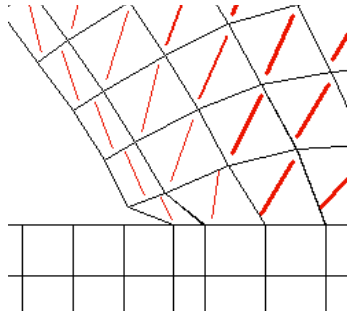


Fig. 4.6. Concrete crushing at compressed toe

The response of models CW-M1 and CW-M3 showed that bond-slip effect was negligible in the control wall response. Both of these models simulated the measured force-displacement response with reasonable accuracy by predicting peak strength and ultimate displacement with 4% and 30% relative error, respectively. The strength deterioration were simulated with acceptable accuracy, but the initial stiffness was overestimated by 26%.

Model CW-M2 in which the tension stiffening effect was neglected to represent the wall response under dynamic loading (Luu et al. 2013), underestimated the strength and initial stiffness by 8% and 10%, respectively. This model did not exhibit strength deterioration, but predicted self-centering behaviour of the control wall reasonably well. The ultimate displacement capacity exhibited by this model was similar to CW-M1 and CW-M3 models. As discussed earlier, these small differences showed that the pseudo-static cyclic response of the walls can be used to represent their dynamic response.

The larger discrepancy between the measured and calculated response with model CW-M4 (Fig 4.6) with respect to the other three models showed the importance of considering buckling effects in reinforcement. Although a considerable number of shear walls (even those designed according to requirements of current codes) exhibit buckling of the boundary reinforcement (Sritharan et al. 2014), not many models are available to consider the buckling and low-cycle fatigue fracture of boundary reinforcement (Jiang and Kurama, 2010). The Akkaya model used in this study showed acceptable results for this purpose. During the experimental program, the tests were terminated due to the significant drop in stiffness and strength of the specimens after post-yield bar buckling, while the analysis predicted concrete crushing at the onset of failure. It should be noted that the buckling of bars in compression is generally followed by crushing of the concrete, and the observed

failure mode in models CW-M1, CW-M2 and CW-M3 indicates the buckling failure (Cortés-Puentes and Palermo, 2011; Palermo and Vecchio, 2007).

#### **4.4 Analysis Model for Hybrid FRP-Steel Reinforced Concrete Walls**

The model with the highest correlation with the experimental results (CW-M3) of the steel-reinforced shear wall was taken as the basis to account for the presence of hybrid GFRP-steel reinforcement (termed “hybrid wall”). Two models for hybrid walls were developed to study the effect of the bond-slip mechanism.

##### **4.4.1 Constitutive materials and model development**

The pre-peak and post-peak behaviour of SFRC in compression was defined using the model developed by Lee et al. (2015) as shown in Fig. 4.2. The GFRP was modeled as a brittle perfectly-elastic material with no compressive capacity. In the model HW-M1, perfect bond was assumed between the GFRP bars and the concrete, while in the model HW-M2, a bond-slip mechanism was considered (Gan-Vecchio model). The Gan-Vecchio bond model is the same as the Eligehausen et al. (1983) model for the confined stress-slip relationship, but the unconfined bond stress-slip relationship is described by an ascending non-linear branch, a descending linear branch, and a sustaining residual stress branch (Wong et al. 2013). The program input parameters for modeling the bond were confinement pressure factor, clear cover spacing and number of reinforcement layers, which were calculated based on specimen details and the confining pressure using Mander et al. model (1988). Other material models and analysis assumptions were similar to the control wall model.

##### **4.4.2 Model validation**

The calculated force-displacement response of HW-M1 and HW-M2 models are presented in Fig. 4.7. The models exhibited toe crushing at their ultimate displacement, which indicated buckling failure as discussed for the control wall models. Model HW-M1 predicted the initial stiffness accurately (1% error), but overestimates the measured strength and displacement capacity by 30%. This model showed better self-centering behaviour than the tested specimen, and it failed to capture the flat plateau observed in the backbone curve of the hybrid wall response.

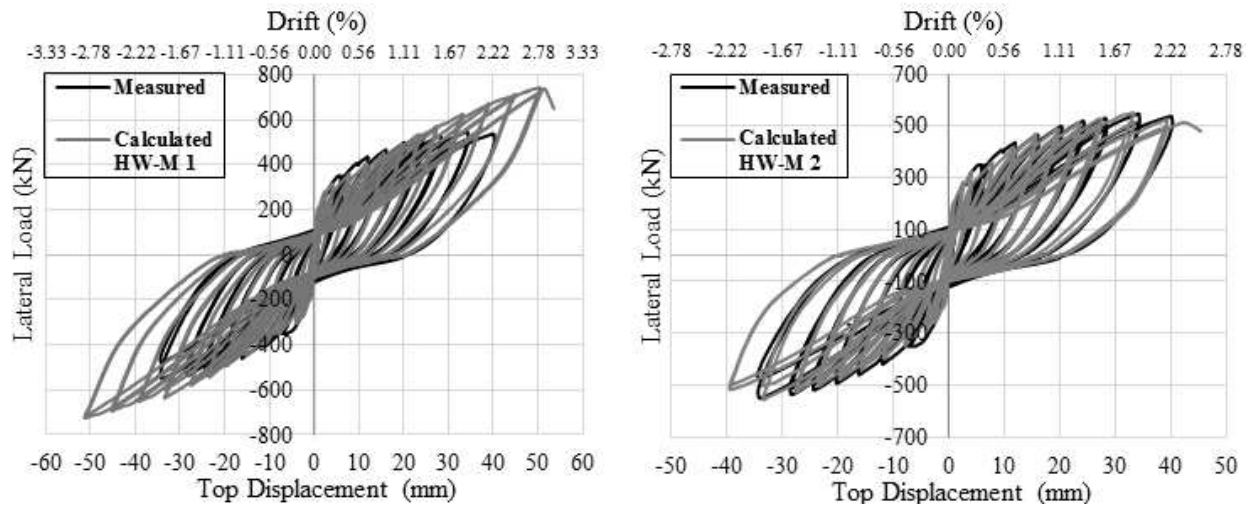


Fig. 4.7. Force-displacement response of HW-M1 and HW-M2 models

The response of Model HW-M2 showed the importance of bond slip modeling in FRP reinforced walls. This model simulated the response of hybrid wall accurately (Fig. 4.7), by predicting the strength, displacement capacity and stiffness with less than 1% error. The hysteretic cycles and self-centering of this model matched the test observations very well.

When designing FRP-steel hybrid members, the amount and location of FRP reinforcement required must be carefully chosen to avoid early rupture of the FRP bars before concrete crushing. To investigate the ability of the model to predict this rupture, measured and calculated tensile strains at the base of GFRP bars are presented in Fig. 4.8, which showed reasonable correspondence between measured and calculated results.

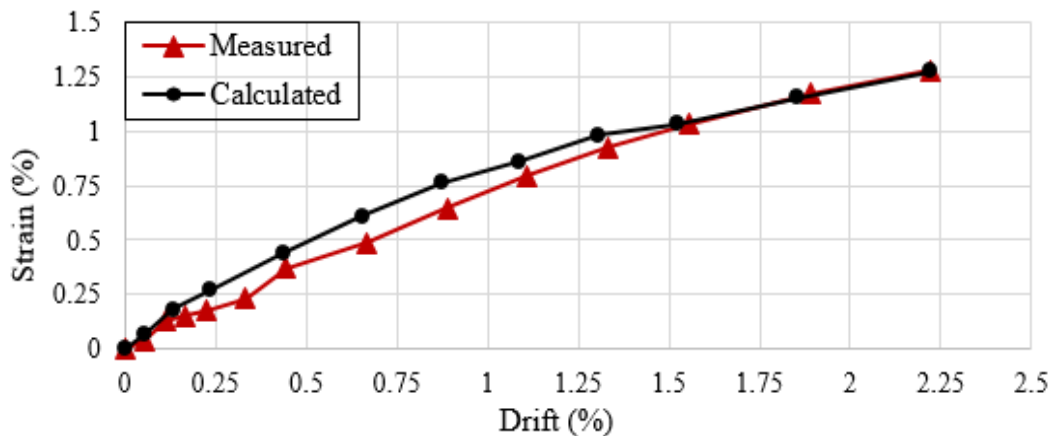


Fig. 4.8. Tensile strains at the base of GFRP bars

Studies on analytical modeling of SFRC walls are scarce up to now (to the authors' knowledge). The presented model showed that by implementing the uniaxial constitutive response of fibre-reinforced concrete into the model, test results can be captured decently.

## **4.5 Parametric Study**

The analysis model was used to investigate the effect of several reinforcement arrangements in low-rise hybrid walls, reinforced with both SFRC and GFRP-steel reinforcement. These models provide behavioural insight and important response parameters for further studies and design applications.

### **4.5.1 FRP reinforcement**

In model Trial1, the #6 GFRP bars of the hybrid wall were replaced with #8 (25 mm) GFRP bars as shown in Fig. 4.9. This is done to explore the convenience of increasing the FRP to steel ratio to obtain higher strength and self-centering capacities. The response of this model under cyclic loading is shown and summarized in Fig. 4.10 and Table 4.2, respectively. By increasing the size of the GFRP bars, the strength of the wall increased by 23%, while the displacement capacity decreased slightly (about 10%) when compared to the hybrid wall (both HW-M2 model and the test results). The displacement capacity decreased since the concrete and boundary reinforcement experienced higher compressive stresses to balance the increased tensile forces in the larger GFRP bars. The failure mode in Trial1 was concrete crushing affected by buckling similar to the hybrid wall. The initial stiffness increase was negligible (2%), but the higher FRP ratio of model Trial1 led to less residual displacements compared to the hybrid wall (from 20 mm to 15 mm in the last hysteretic cycle). As shown in Table 4.2, this model had almost similar energy dissipation capacity to the tested hybrid wall.

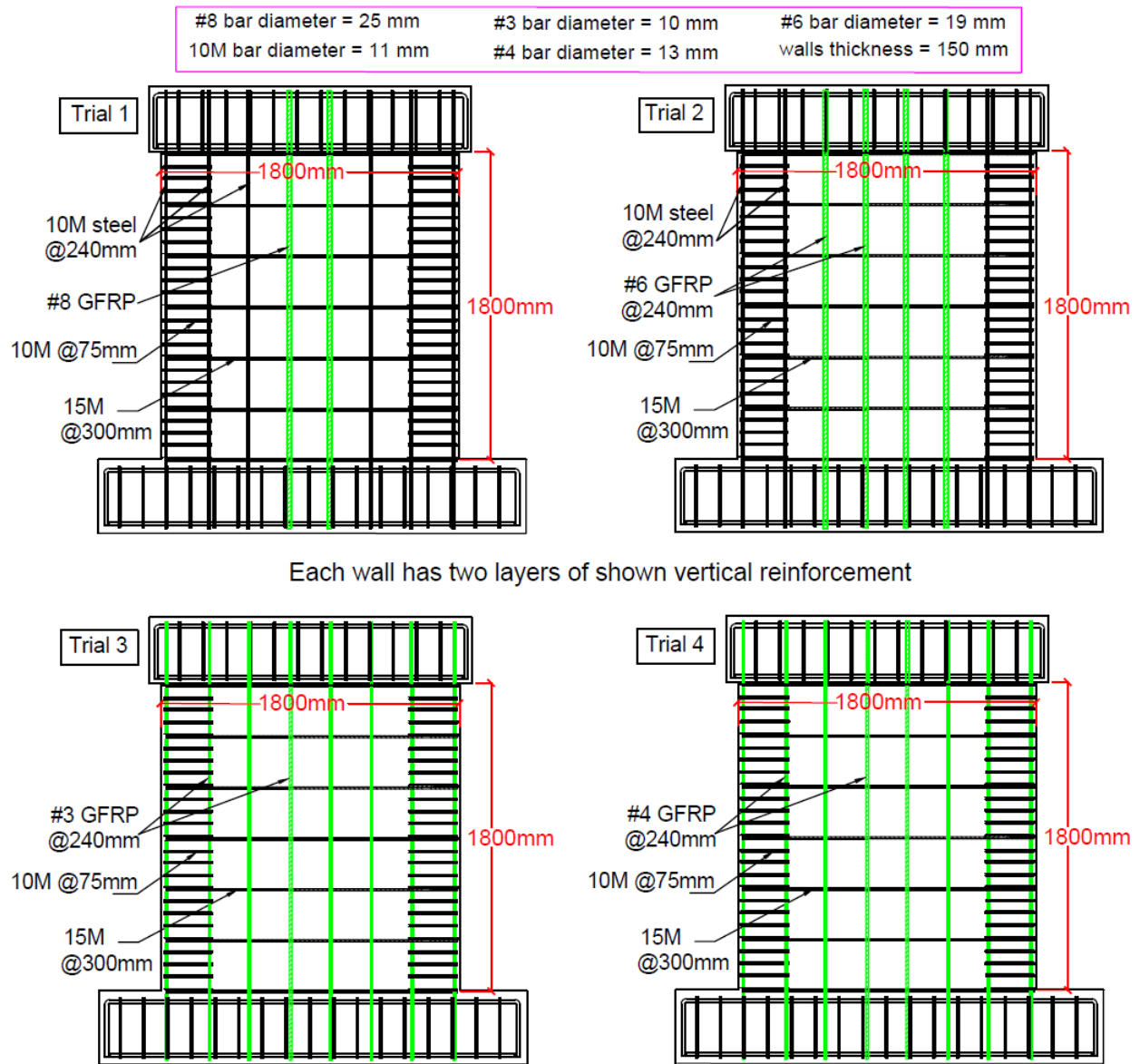


Fig. 4.9. Detailing of the hybrid and GFRP-reinforced models

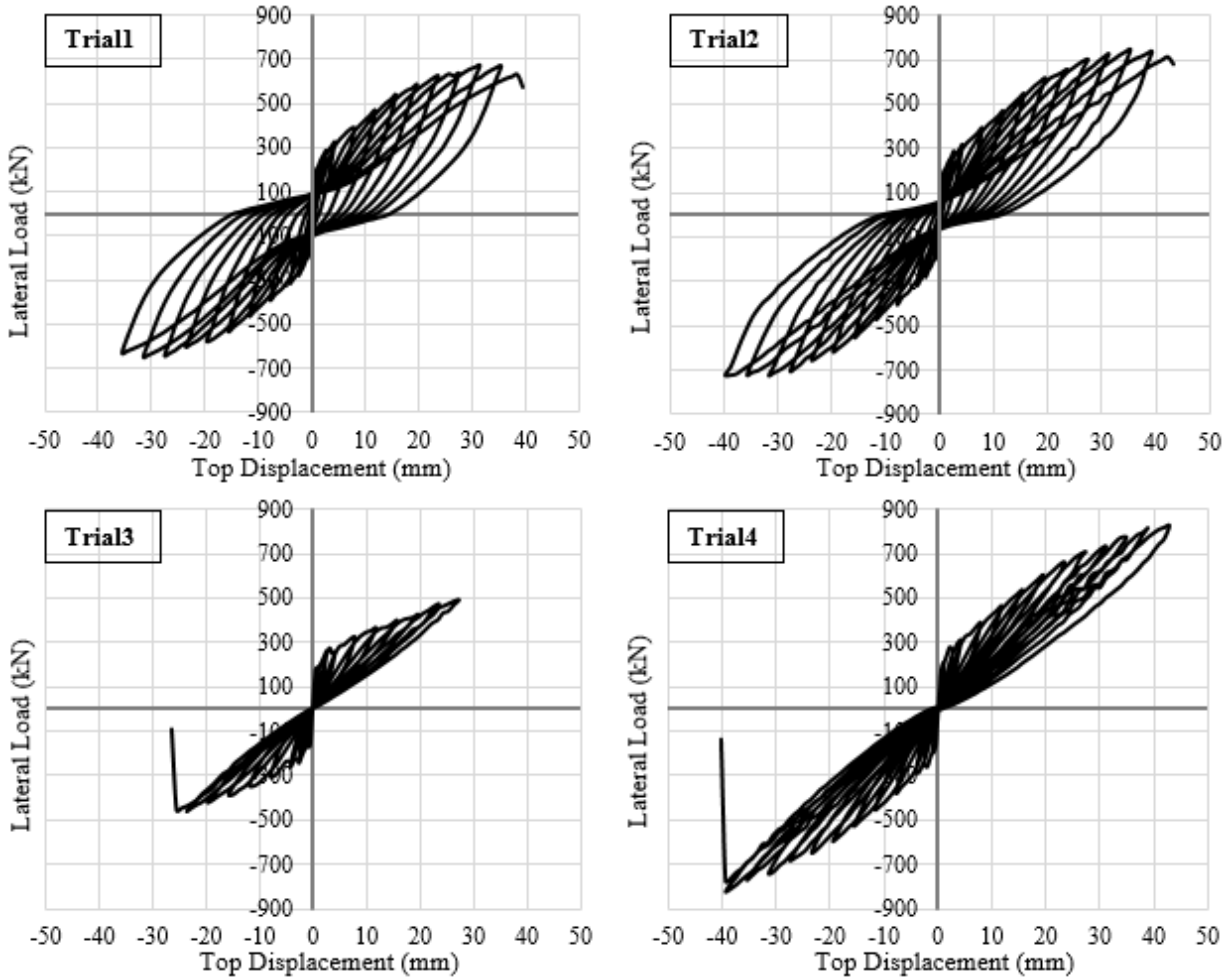


Fig. 4.10. Force-displacement response of the hybrid and GFRP-reinforced models

Table 4.2. Summary of modeling results for the hybrid and GFRP-reinforced models

Models	Peak lateral load (kN)	Ultimate displacement (mm)	Maximum residual displacement (mm)	Initial stiffness (kN/mm)	Dissipated energy (area enclosed in last cycle) (kN.m)
<b>Trial1</b>	676	36	15	204	17.8
<b>Trial2</b>	746	40	11	201	17.4
<b>Trial3</b>	488	28	0	177	1.7
<b>Trial4</b>	821	40	0	199	5.9
<b>HW-M2</b>	549	40	20	201	20.1
<b>Test- Hybrid wall</b>	550	40	20	200	21.3
<b>Test- Control wall</b>	588	40	25	207	19.7

In Trial2 model, the web reinforcement of the hybrid wall were replaced with #6 GFRP bars as shown in Fig. 4.9. Despite placing the FRP bars closer to the wall boundaries than in hybrid wall, fracture of the GFRP bars did not occur before buckling of the boundary steel bars and crushing of the confined concrete, which is a desirable design target for elements that contain FRP

reinforcement. Trial2 had similar displacement capacity and initial stiffness to the hybrid wall, while having 35% higher flexural strength. The maximum residual displacement observed in this wall was 11 mm. Despite the reduction in the amount of steel reinforcement, this wall had comparable energy dissipation capacity to the control wall and the hybrid wall.

Trial3 and Trial4 were exclusively reinforced with GFRP bars of different sizes, #3 (10 mm) and #4 (13 mm) bars respectively, as shown in Fig. 4.9. The hysteretic response (Fig. 4.10) showed that these walls did not experience residual displacements, as shown experimentally by Mohamed et al. (2014b) for the walls detailed entirely with GFRP reinforcement. However, their energy dissipation capacity was very small in comparison to the hybrid FRP-steel reinforced walls. The response of the hybrid walls (Trial1 and Trial2) was more desirable since input energy of earthquakes are expected to be dissipated in the hysteretic cycles. In model Trial3, which was reinforced with #3 bars, rupture of GFRP bars occurred at an early displacement (28 mm). The strength and initial stiffness of this wall were 12% less than the hybrid wall. Trial4 wall failed at displacement of 40 mm due to rupture of the GFRP bars. This model had 50% higher flexural strength than the hybrid wall while having the same initial stiffness. The model with smaller GFRP reinforcement ratio (Trial3) failed at a smaller ultimate displacements since the boundary bars reached their ultimate strength sooner than in wall with higher GFRP reinforcement ratio (Trial4). In steel-reinforced walls, lightly reinforced walls yield sooner than walls with high reinforcement ratios due to the same reason.

#### **4.5.2 Steel fibre-reinforced concrete (SFRC)**

As discussed in details in the companion study (chapter 3), the code recommendations (ACI 2014; CSA 2014) for the spacing of buckling prevention ties were not followed to evaluate the potential of confinement reinforcement elimination by use of fibre-reinforced concrete. This idea was first suggested by Athanasopoulou and Parra-Montesinos (2013) in the research done on shear walls with SFRC. The experimental results obtained in this study showed that presence of fibres can not prevent buckling of the bars.

In Trial5 and Trial6 models, the spacing of confinement ties in the control wall model (CW-M3) and hybrid wall model (HW-M2) were adjusted to meet the code provisions for buckling prevention, as shown in Fig. 4.11. Trial5 model, in which the buckling prevention ties were added to the control wall, had 15% higher displacement capacity (Fig. 4.12) than the control wall model

(CW-M3). When the buckling prevention ties added to the hybrid wall (Trial6), in addition the displacement capacity, strength of the wall increased by 17% as well (Fig. 4.12), due to the elastic response of GFRP bars. The response of Trial5 and Trial6 models showed that meeting the buckling prevention requirements in current codes of practice would translate into a comparable increment in displacement capacity in both types of wall.

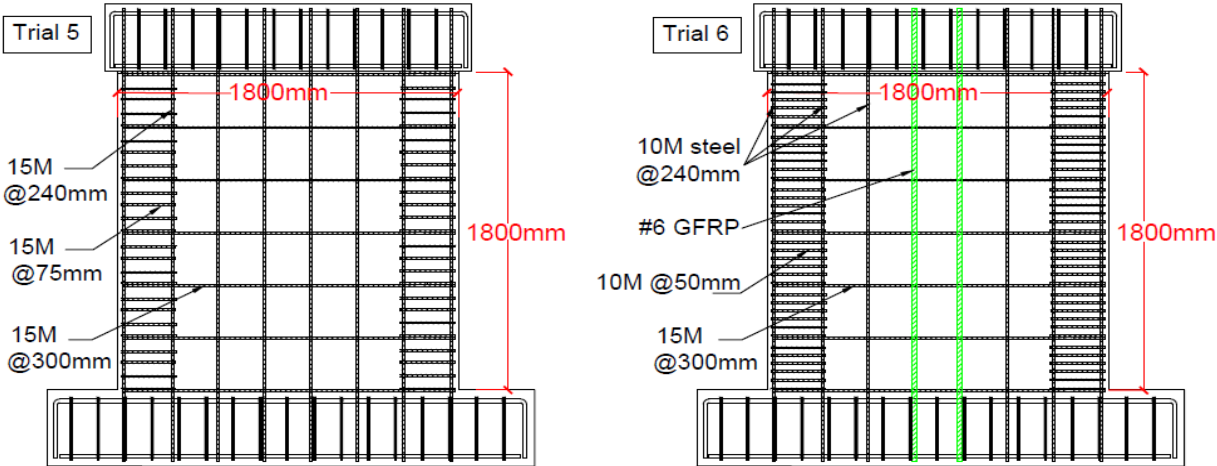


Fig. 4.11. Detailing of Trial5 and Trial6 models

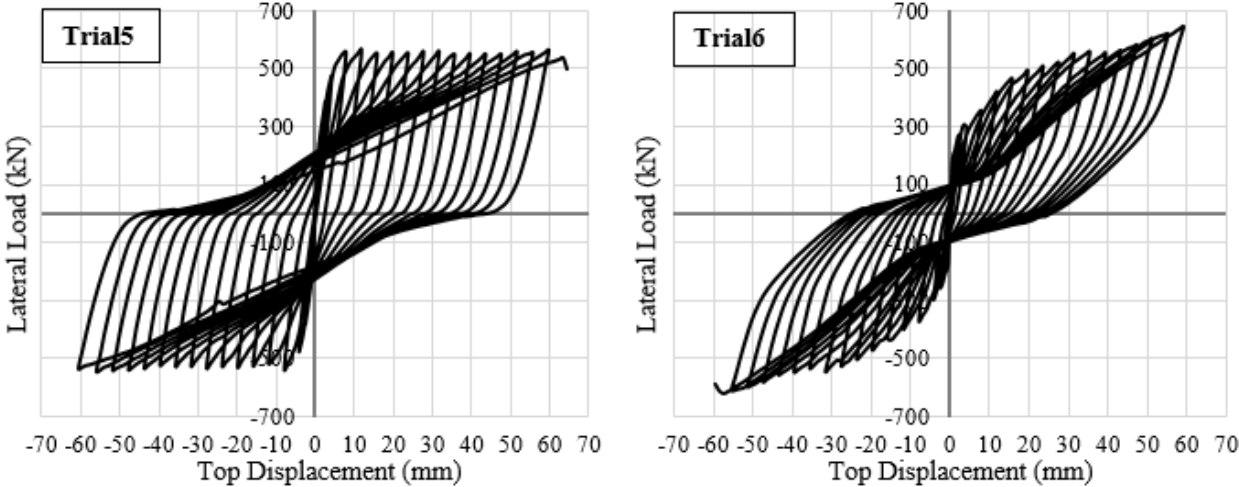


Fig. 4.12. Force-displacement response of Trial5 and Trial6 models

To study the potential usage of SFRC, two steel-reinforced shear walls were designed according to code provisions, a moderately-reinforced specimen (Trial7) and a heavily-reinforced one (Trial8) as shown in Fig. 4.13. Geometry and material properties of these two models were similar

to the control wall. Both walls, with a higher amount of steel reinforcement than the control wall, exhibited a flexural failure mode characterized by concrete crushing after steel yielding, with the cyclic response shown in Fig. 4.14.

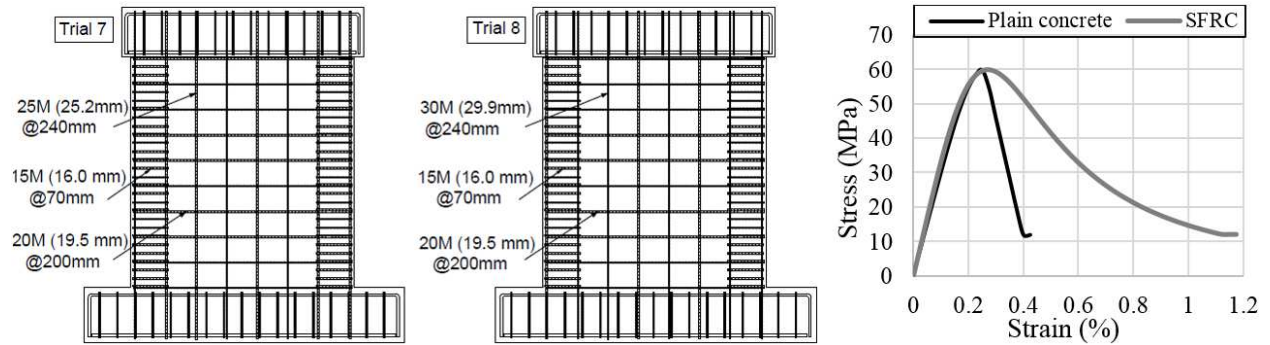


Fig. 4.13. Detailing and concrete behaviour of Trial7 and Trial8 models

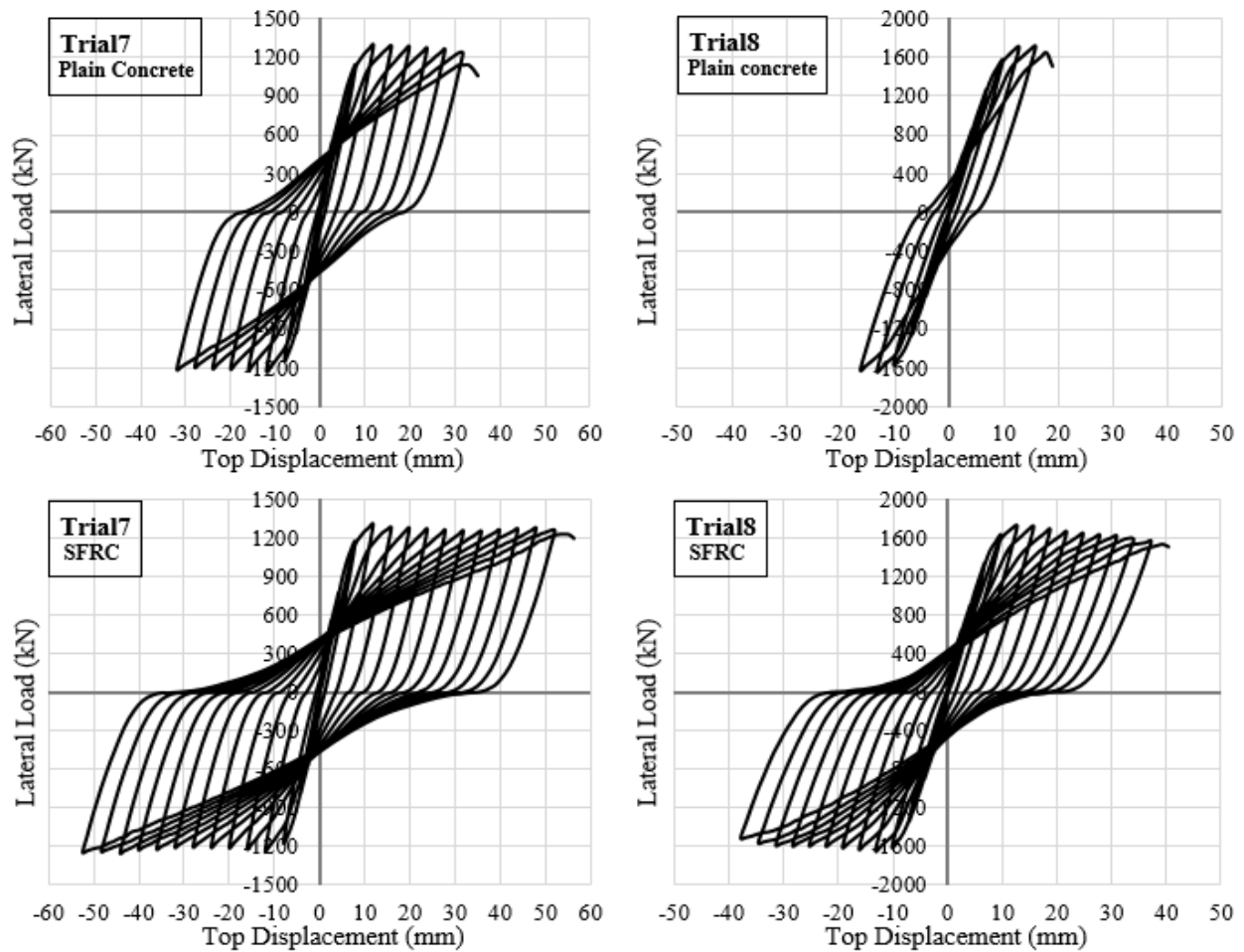


Fig. 4.14. Force-displacement response of Trial7 and Trial8 models with and without fibres

Comparing the response of model Trial5 (the control wall model with closely spaced boundary ties) and the models Trial7 and Trial8, it is seen that by increasing the amount of vertical reinforcement, the displacement capacity of the walls decreased significantly. This was expected since the concrete in compression experienced higher compressive stresses to balance the larger tensile forces in the walls with high steel reinforcement ratio. Next, the normal-weight concrete of Trial7 and Trial8 models were replaced with SFRC of the same strength, with the compressive response shown in Fig. 4.13. With the addition of fibres, the displacement capacity of Trial7 and Trial8 models increased by 66% and 111%, respectively. The calculated energy dissipation capacity of Trial7 and Trial8 models with fibres were 74% and 239% higher than the models with normal-weight concrete. These results are promising since it would allow engineers to design and build ductile low-rise walls. Usage of SFRC is also suggested for the condition of presence of high compressive axial loads, which decreases rotational ductility and displacement capacity of walls significantly (Su and Wong, 2006).

Uniaxial tensile stress-strain response of SFRC cylinders were not measured during the experimental program due to the restrictions in lap equipment. On the other hand, uniaxial tensile behaviour cannot be defined manually in concrete models of current version of VecTor2. Thus, crack bridging and post-cracking tensile strength of SFRC was neglected in the model. The effect of this assumption was observed to be negligible using cross-section analysis and modeling results. Zhao et al. (2014) showed that the ultimate point of slender SFRC shear walls can be identified using cross-section analysis with reasonable accuracy. In the section analysis conducted for the hybrid wall, two scenarios were evaluated: no post-cracking tensile strength, and with constant post-cracking tensile strength up to a strain of 1% based on the experimental study done by Kim et al. (2014). When considering the post-cracking tensile strength, the capacity of the wall increased by 16 kN.m and the neutral axis depth changed by 30 mm which are negligible. The validation of the FE model also showed that neglecting post-cracking tensile response of SFRC has insignificant effect on behaviour of the walls experiencing a compressive failure consisting concrete crushing or rebar buckling. Prior to cracking, the response was assumed to be linear elastic.

### 4.5.3 Concrete strength

As discussed in chapter 3, the concrete mix provided for the hybrid wall by the supplier had a lower compressive strength than the control wall. Using the analysis model, response the hybrid specimen having SFRC with compressive strength of 60 MPa was predicted. As shown in Fig. 4.15, the response was very similar to the tested specimen; Self-centering and displacement capacity were the same and strength of the walls increased to 600 kN (50 kN increase).

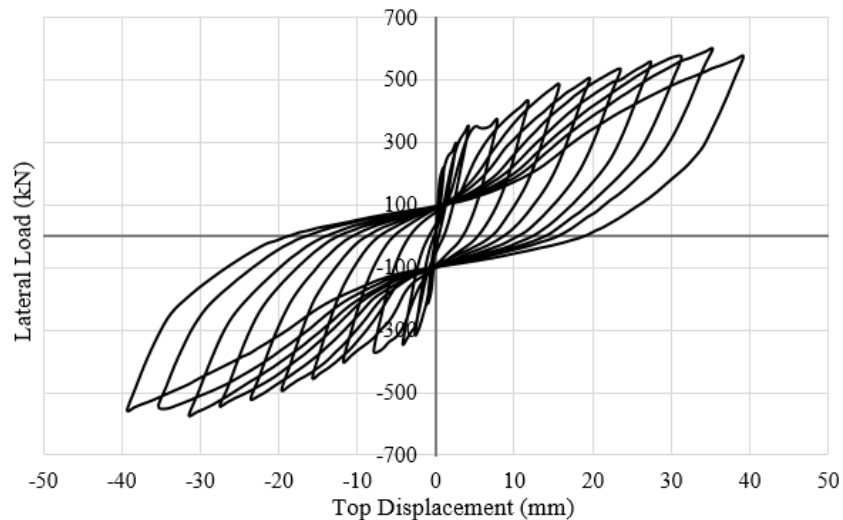


Fig. 4.15. Force-displacement response of hybrid wall with 60 MPa SFRC

### 4.5.4 Axial load

Previous research has shown that axial compressive loads would improve self-centering behaviour of the walls (Maciel et al. 2016). As it was desired to study the effects of self-centering provided exclusively by the GFRP bars, no gravity load was applied to the specimens. It worth to note that low-rise walls with negligible axial load ratios can be found in real-life construction (Looi et al. 2017). However, using the analysis model, response of the walls under three different axial loads were studied. Compressive loads of 270 kN, 540 kN, and 810 kN which correspond to 2.5%, 5% and 7.5% of hybrid wall axial capacity (area  $\times$  compressive strength) were applied to both walls. Predicted responses are shown in Fig. 4.16. These axial loads decreased displacement capacity and increased strength and self-centering behaviour of the walls. In the control wall, the improvement in self-centering behaviour was slight and a residual displacement of 18 mm was observed even under 810 kN axial load, while the same self-centering ratio (0.50) was observed in the hybrid wall

without axial load. Improvement of self-centering behaviour was significant in the hybrid models. Residual displacement was reduced to 13 mm in presence of 270 kN compressive load in the hybrid wall, while negligible residual displacements were observed for higher axial loads.

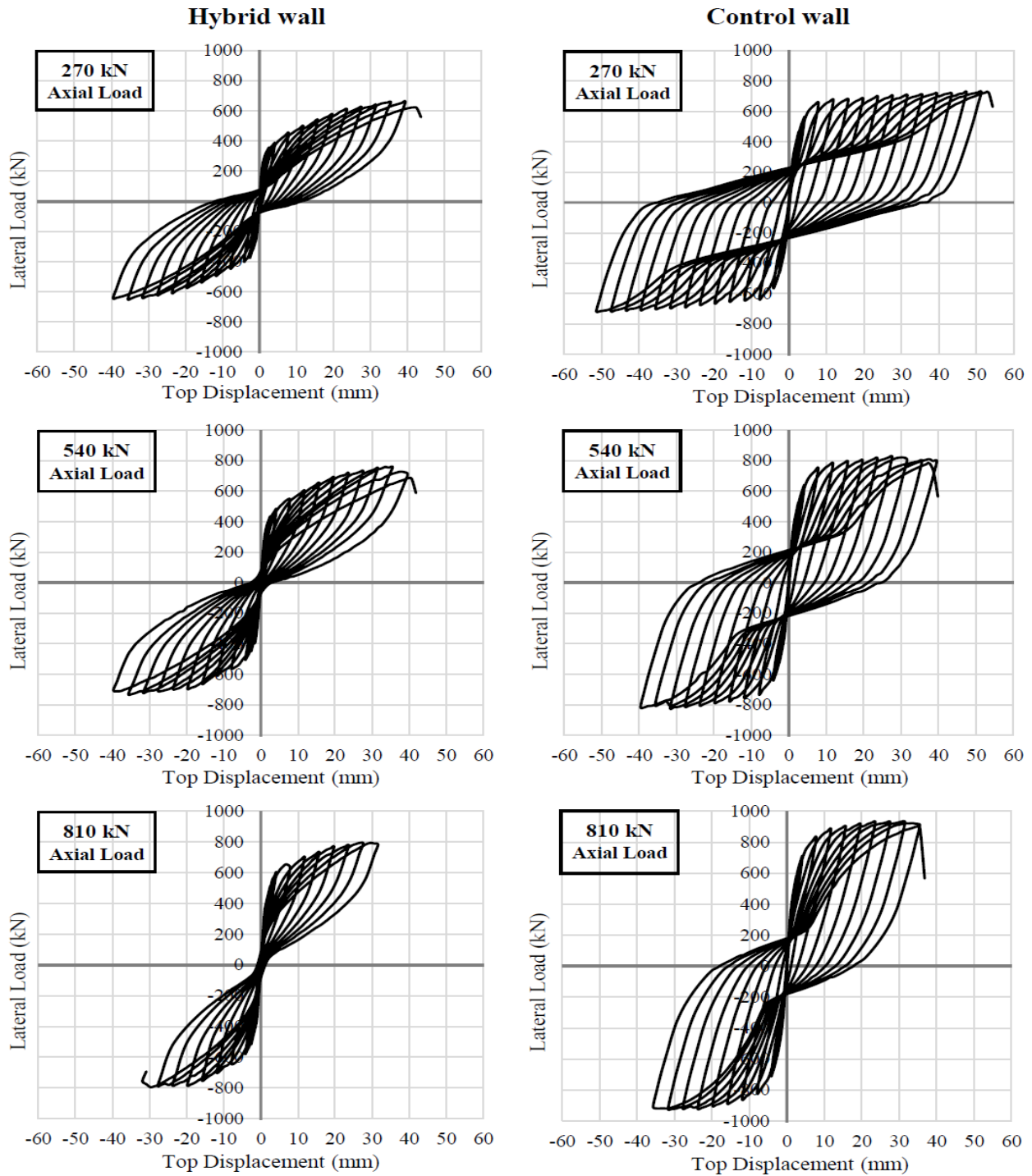


Fig. 4.16. Force-displacement response of the walls under different axial loads

## 4.6 Importance and Applications

Response of shear walls as the members that provide lateral strength and stiffness in concrete structures, have a significant influence on amount of residual interstorey drifts of a building after an earthquake (Ramirez and Miranda, 2012). To study the importance of these residual displacements, Ramirez and Miranda (2012) estimated the economic losses in terms of observed residual drifts. Fig. 4.17 shows the probability of having to demolish a building that has not collapsed as a function of the peak residual interstorey drift in a building. This probability is zero up to 0.8% drifts and small amount of residual drifts do not lead to high post-earthquake costs. Since different parameters such as height and displacement capacity of a wall would affect its residual drifts, deciding about the adequacy of tested walls in terms of presented probability would not be reasonable. However, results of current study show that the proposed hybrid system can be used to avoid demolition and replacement costs by reducing exhibited residual displacements.

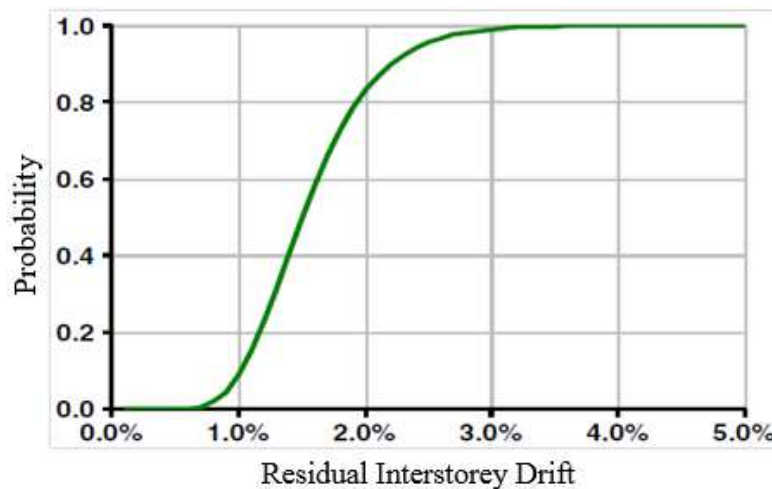


Fig. 4.17. Probability of having to demolish a building (Ramirez and Miranda, 2012)

## 4.7 Conclusions

In this study, an analysis model for hybrid FRP-steel reinforced shear walls and SFRC walls is developed and validated with experimental results. The model is used to investigate the response of several configurations of reinforcement in low-rise walls in terms of strength, stiffness,

displacements and energy dissipation. The following conclusions can be drawn from this investigation:

- The nonlinear response of low-rise walls, which is associated with nonlinear flexural and shear deformations, can be simulated with decent accuracy using the proposed model. It is shown that the model provides satisfactory prediction of the experimentally-measured cyclic response of the specimen reinforced with hybrid GFRP-steel bars and fibre-reinforced concrete, including the strength, ultimate displacement, stiffness degradation, energy dissipation and self-centering behaviour of the wall. This analysis model is able to take into account the reinforcement buckling and bond-slip effects. However, more advanced models are needed to capture the fracture of buckled reinforcement due to loading and unloading cycles.
- In hybrid GFRP-steel low-rise walls, an arrangement of GFRP bars at the middle region is desirable, since it translates into a ductile mode of failure consist of concrete crushing after substantial yielding of boundary steel, with no rupture of GFRP bars. The hybrid system exhibits significantly less residual displacements than its RC counterpart. Although the self-centering capacity in hybrid walls is less than the walls reinforced entirely with FRP bars, hybrid walls have higher stiffness and energy dissipation capacity.
- Axial compressive loads improve self-centering behaviour of steel-reinforced walls slightly, while significant self-centering behaviour in response of hybrid walls is observed with presence of axial loads. An experimental study can be conducted in future to validate this issue and address the mechanism.
- Considering a perfect bond between the concrete and GFRP bars could be potentially unsafe since a higher strength and better self-centering behaviour is predicted. More studies are needed to improve the bond strength of GFRP bars to concrete, and use the FRP bars in a more effective way.
- Heavily-reinforced low-rise wall may have limited displacement capacity, even those designed according to the seismic codes. The analysis results show that the displacement capacity and energy dissipation capacity of such walls can be improved significantly by usage of fibre reinforced concrete. However, lack of experimental data on this type of walls is a major drawback.

As discussed, the innovative hybrid system can be considered as a promising alternative to conventional RC construction. The presented model can be used to address design aspects and develop guidelines for practical application of the proposed system.

## **CHAPTER 5 SUMMARY, CONCLUSIONS AND FUTURE WORK**

An experimental program investigating the response of two low-rise shear walls under cyclic, lateral-loading and a series of numerical simulations are conducted in this research to study an innovative system for construction of shear walls: low-rise shear walls with hybrid FRP-steel vertical reinforcement and steel fibre-reinforced concrete. First specimen is a conventional steel-reinforced concrete (RC) shear wall with height-to-length ratio of 1, designed as the seismic considerations of the CSA A23.3-14 and ACI 318-14 codes with a relaxation in confinement reinforcement. Second specimen is an innovative wall with hybrid GFRP-steel vertical reinforcement and steel fibre-reinforced concrete (SFRC). The overall research conclusions and recommendations for further work are as the following:

- In hybrid FRP-steel low-rise walls, an arrangement of FRP bars at the middle region of the wall together with steel bars at the wall boundaries is able to achieve comparable strength, stiffness and ductility with conventional RC walls under static cyclic loading. With such arrangement of vertical reinforcement, it is shown that the rupture of FRP bars can be avoided while outer steel bars exhibit significant yielding before member failure.
- The seismic performance of an appropriately designed hybrid FRP-steel reinforced wall is shown to be comparable to RC members in terms of displacements. However, the hybrid system has improved self-centering behaviour in comparison to its RC counterpart, while maintaining a significant energy dissipation capacity. Better self-centering behaviour can be obtained by increasing the amount of FRP reinforcement. This helps to avoid the excessive residual displacements that can result in high repair costs after earthquakes.
- Backbone curves of hybrid walls force-displacement response show a characteristic tri-linear behaviour, in which the uncracked, cracked and yielded state of the walls can be readily identified. The backbone curves are not associated with capacity deterioration, which makes the hybrid walls suitable for a performance-based design. The service limit state in hybrid walls

can be met by adding more steel at the wall boundaries, while the slope of yielded state is controlled by FRP reinforcement.

- The nonlinear response of low-rise walls, which is associated with nonlinear flexural and shear deformations, can be simulated with decent accuracy using the proposed model. It is shown that the model provides satisfactory prediction of the experimentally-measured cyclic response for the specimen reinforced hybrid GFRP-steel bars and fibre-reinforced concrete, including the strength, ultimate displacement, stiffness degradation, energy dissipation and self-centering behaviour of the wall.
- Although the literature has suggested that usage of SFRC would increase the drift capacity and allow relaxation of confinement reinforcement in the walls, fibres are not able to delay buckling of longitudinal bars. Therefore, the proposed relaxation is not feasible in cases that buckling of boundary bars are critical. However, usage of SFRC in shear walls increases the post-cracking damage tolerance.
- The improved analysis model presented in chapter 4 is able to take into account the reinforcement buckling and bond slip effects. However, more advanced models are needed to capture the fracture of buckled reinforcement due to loading and unloading cycles.
- Axial compressive loads improve self-centering behaviour of steel-reinforced walls slightly, while significant self-centering behaviour in response of hybrid walls is observed with presence of axial loads. An experimental study can be conducted in future to validate this issue and address the mechanism.
- Modeling results show that better self-centering and higher strength can be achieved by a better bond between the GFRP bars and concrete. Therefore, further studies can be conducted to improve the bond strength between the GFRP bars and concrete.
- Modeling results show that the displacement capacity and energy dissipation capacity of heavily-reinforced low-rise walls can be improved significantly by usage of fibre reinforced concrete. However, experimental studies are needed to validate and address this issue appropriately. This allows the engineers to design low-rise walls with higher ductility, which ends to a lighter and more economic design. Also more studies can be conducted to address the potential of SFRC to increase the shear capacity of shear walls.
- More advanced models are needed to consider the exact tensile behaviour of SFRC. Although it is shown that tensile behaviour of SFRC has negligible effect on overall load-displacement

response of the walls studied in the current research, it may be crucial in the walls with different aspect ratios or walls that exhibit a shear failure mode.

Advantages and disadvantages of usage of hybrid FRP-steel reinforcement and fibre-reinforced concrete in low-rise shear walls are discussed in this study. The proposed innovative systems have the potential to be considered as an alternative to conventional RC construction.

## REFERENCES

Adorno-Bonilla, C. M., Vidot-Vega, A. L., and Miranda, M. (2014). "Tools for modeling the lateral response of squat reinforced concrete shear walls." *10th U.S. National Conference on Earthquake Engineering*, Anchorage, AK, USA.

American Concrete Institute (ACI). (2014). "Building code requirements for structural concrete (ACI 318-14) and commentary (318 R-14)." *ACI Committee 318*, Farmington Hills, MI, USA.

Athanasopoulou, A. (2010). "Shear strength and drift capacity of reinforced concrete and high-performance fiber reinforced concrete low-rise walls subjected to displacement reversals." Doctoral dissertation, Dept. of Civil and Environmental Engineering, University of Michigan, Ann Arbor, MI, USA.

Athanasopoulou, A., and Parra-Montesinos, G. (2013). "Experimental study on the seismic behavior of high-performance fiber-reinforced concrete low-rise walls." *ACI Struct. J.*, 110(5), 767.

Campione, G. (2011). "Compressive behavior of short fibrous reinforced concrete members with square cross-section." *Struct. Eng. Mech.*, 37(6), 649-669.

Canadian Standards Association (CSA). (2012). "Design and construction of building components with fibre-reinforced polymer." *CAN/CSA-S806-12*, Rexdale, ON, Canada.

Canadian Standards Association (CSA). (2014). "Design of concrete structures." *CAN/CSA A23.3-14*, Mississauga, ON, Canada.

Carrillo, J., and Alcocer, S. M. (2012). "Backbone model for performance-based seismic design of RC walls for low-rise housing." *Earthquake Spectra*, 28(3), 943-964.

Carrillo, J., Alcocer, S. M., and Pincheira, J. (2012). "Shaking table tests of steel fiber reinforced concrete walls for housing." *15th World Conference on Earthquake Engineering*, Lisbon, Portugal.

Cortes-Puentes, W. L., and Palermo, D. (2011). "Modelling seismically repaired and retrofitted reinforced concrete shear walls." *Comput. & Concr.*, 8(5), 541-561.

Cruz-Noguez, C., Lau, D., and Sherwood, E. (2012). "Analytical modeling of reinforced concrete shear walls with externally-bonded CFRP reinforcement." *6th International Conference on Advanced Composite Materials in Bridges and Structures (ACMBS-VI)*, p.22-25.

Cruz-Noguez, C., Lau, D., and Sherwood, E. (2014a). "Seismic behavior of RC shear walls with externally bonded FRP sheets: analytical studies." *J. Compos. Constr.*, 10.1061/(ASCE)CC.1943-5614.0000466, 04014011.

Cruz-Noguez, C., Lau, D., Sherwood, E., Hiotakis, S., Lombard, J., Foo, S., and Cheung, M. (2014b). "Seismic behavior of RC shear walls strengthened for in-plane bending using externally bonded FRP sheets." *J. Compos. Constr.*, 10.1061/(ASCE)CC.1943-5614.0000478, 04014023.

Eligehausen, R., Popov, E. P., and Bertero, V. V. (1983). "Local bond stress-slip relationships of deformed bars under generalized excitations." *Rep. No. UCB/EERC-83/23*, Univ. of California, Berkeley, CA, USA.

Erkmen, B. and Schultz, A. E. (2009). "Self-centering behavior of unbonded, post-tensioned precast concrete shear walls." *J. Earthq. Eng.*, 13(7), 1047-64.

Filiatrault, A., Restrepo, J., and Christopoulos, C. (2004). "Development of self-centering Earthquake resisting systems." *13th World Conference on Earthquake Engineering*, Vancouver, BC, Canada.

Fischinger, M., Rejec, K., and Isaković, T. (2012). "Modeling inelastic shear response of RC walls." *Proc., 15th World Conference on Earthquake Engineering*, Lisbon, Portugal.

Ghazizadeh, S., Talaei, F., and Cruz-Noguez, C. A. (2016). "Analysis model for hybrid GFRP-steel reinforced shear walls." *Proceedings of the 7<sup>th</sup> International Conference on Advanced Composite Materials in Bridges and Structures*, Vancouver, BC, Canada.

Gulec, C. K., and Whittaker, A. S. (2009). "Performance-based assessment and design of squat reinforced concrete shear walls." *Technical Rep. MCEER-09-0010*, New York Univ. at Buffalo, Buffalo, NY, USA.

Hidalgo, P. A., Ledezma, C. A., and Jordan, R. M. (2002). "Seismic behavior of squat reinforced concrete shear walls." *Earthquake Spectra*, 18(2), 287-308.

Jakubovskis, R., Kaklauskas, G., Gribniak, V., Weber, A., and Juknys, M. (2014). "Serviceability analysis of concrete beams with different arrangements of GFRP bars in the tensile zone." *J. Compos. Constr.*, 10.1061/(ASCE)CC.1943-5614.0000465, 04014005.

Jiang, H., and Kurama, Y. C. (2010). "Analytical modeling of medium-rise reinforced concrete shear walls." *ACI Struct. J.*, 107(4), 400-410.

Kang, S. W., and Yun, H. D. (2013). "Effect of cement matrix's type on the shear performance of lightly reinforced squat shear walls subjected to cyclic loading." *Adv. Mater. Res.*, 658, 42-45.

Kharal, Z. (2014). "Tension Stiffening and Cracking Behaviour of GFRP Reinforced Concrete." Ph.D. dissertation, Dept. of Civil Engineering, Univ. of Toronto, Toronto, ON, Canada.

Kim, J. J., Park, G. J., Kim, D. J., Moon, J. H., and Lee, J. H. (2014). "High-rate tensile behavior of steel fiber-reinforced concrete for nuclear power plants." *Nucl. Eng. Des.*, 266, 43-54.

Kolozvari, K. (2013). "Analytical modeling of cyclic shear-Flexure interaction in reinforced concrete structural walls." Ph.D. dissertation, Dept. of Civil Engineering, Univ. of California, Los Angeles, CA, USA.

Kolozvari, K., Orakcal, K., and Wallace, J. (2014a). "Modeling of cyclic shear-flexure interaction in reinforced concrete structural walls. I: Theory." *J. Struct. Eng.*, 10.1061/(ASCE)ST.1943-541X.0001059, 04014135.

Kolozvari, K., Tran, T., Orakcal, K., and Wallace, J. (2014b). "Modeling of cyclic Shear-flexure interaction in reinforced concrete structural walls. II: Experimental validation." *J. Struct. Eng.*, 10.1061/(ASCE)ST.1943-541X.0001083, 04014136.

Krall, M. (2014). "Tests on concrete beams with GFRP flexural and shear reinforcements & analysis method for indeterminate strut-and-tie models with brittle reinforcements." Master's thesis, Dept. of Civil and Environmental Engineering, University of Waterloo, Waterloo, ON, Canada.

Kupfer, H., Hilsdorf, H. K., and Rusch, H. (1969). "Behavior of concrete under biaxial stresses." *ACI J.*, 66(8), 656-666.

Lee, M. K., and Barr, B. I. G. (2004). "An overview of the fatigue behaviour of plain and fibre reinforced concrete." *Cem. Concr. Compos.*, 26(4), 299-305.

Lee, S. C., Oh, J. H., and Cho, J. Y. (2015). "Compressive behavior of fibre-reinforced concrete with end-hooked steel fibres." *Materials*, 8(4), 1442-1458.

Liu, R. (2011). "Precast concrete bridge deck panels reinforced with glass fiber reinforced polymer bars." Doctoral dissertation, Dept. of Civil and Environmental Engineering, University of Utah, Salt Lake City, UT, USA.

Looi, D. T. W., Su, R. K. L., Cheng, B., and Zhou, M. J. (2016). "Ultimate drift prediction models of rectangular squat reinforced concrete shear walls." *Mech. Struct. Mater.: Advancements and Challenges*, 1653-1660, in press.

Luu, H., Ghorbanirenani, I., Léger, P., and Tremblay, R. (2013). "Numerical modeling of slender reinforced concrete shear wall shaking table tests under high-frequency ground motions." *J. Earthq. Eng.*, 17(4), 517-542.

Maciel, M., Palermo, D., and Abdulridha, A. (2016). "Seismic Response of SMA Reinforced Shear Walls." *Special Topics in Structural Dynamics*, 6, 185-192.

Mander, J. B., Priestley, M. J., and Park, R. (1988). "Theoretical stress-strain model for confined concrete." *J. Struct. Eng.*, 114(8), 1804-1826.

Massone, L. M., Orakcal, K., and Wallace, J. W. (2006). "Shear-flexure interaction for structural walls." *ACI special publication SP-236-07—Deformation capacity and shear strength of reinforced concrete members under cyclic loading*, 236, 127-150.

Mazzoni, S., McKenna, F., Scott, M. H., and Fenves, G. L. (2006). "OpenSees command language manual." *Pacific Earthquake Engineering Research Center*, Univ. of California, Berkeley, CA, USA.

McKenna, F., Fenves, G. L., and Scott, M. H. (2000). "Open system for earthquake engineering simulation." *Pacific Earthquake Engineering Research Center*, Univ. of California, Berkeley, CA, USA, {<http://OpenSees.berkeley.edu>}.

Mohamed, N. A. A. (2013). "Strength and drift capacity of GFRP-reinforced concrete shear walls." Doctoral dissertation, Dept. of Civil and Environmental Engineering, Univ. of Sherbrooke, QC, Canada.

Mohamed, N., Farghaly, A. S., Benmokrane, B., and Neale, K. (2014a). "Drift capacity design of shear walls reinforced with glass fiber-reinforced polymer bars." *ACI Struct. J.*, 111(6), 1397-1406.

Mohamed, N., Farghaly, A. S., Benmokrane, B., and Neale, K. (2014b). "Experimental investigation of concrete shear walls reinforced with glass fiber-reinforced bars under lateral cyclic loading." *J. Compos. Constr.*, 10.1061/(ASCE)CC.1943-5614.0000393, A4014001.

Mohamed, N., Farghaly, A. S., Benmokrane, B., and Neale, K. W. (2014c). "Numerical simulation of mid-rise concrete shear walls reinforced with GFRP bars subjected to lateral displacement reversals." *Eng. Struct.*, 73, 62-71.

Palermo, A., Pampanin, S., Buchanan, A. H., and Newcombe, M. P. (2005). "Seismic design of multi-storey buildings using laminated veneer lumber (LVL)." *New Zealand Society of Earthquake Engineering, Annual Conf.*, Univ. of Canterbury, Civil Engineering, Wairakei, New Zealand.

Palermo, D., and Vecchio, F. J. (2002). "Behaviour and analysis of reinforced concrete walls subjected to reversed cyclic loading." *Publication No. 2002-01*, Dept. of Civil Engineering, Univ. of Toronto, Toronto, ON, Canada.

Palermo, D. and Vecchio, F. J. (2004). "Compression field modeling of reinforced concrete subjected to reversed loading: Verification." *ACI Struct. J.*, 101(2), 155-64.

Palermo, D. and Vecchio, F. J. (2007). "Simulation of cyclically loaded concrete structures based on the finite-element method." *J. Struct. Eng.*, 10.1061/(ASCE)0733-9445(2007)133:5(728), 728-738.

Pang, X. B. D., and Hsu, T. T. (1995). "Behavior of reinforced concrete membrane elements in shear." *Struct. J.*, 92(6), 665-679.

Park, R. (1988). "State of the art report: ductility evaluation from laboratory and analysis testing." *Proceeding of Ninth World Conference on Earthquake Engineering*, Tokyo-Kyoto, Japan.

"PEER strong motion database." (2016). {<http://peer.berkeley.edu>} (Accessed Mar. 21, 2016).

Petrangeli, M., Pinto, P., and Ciampi, V. (1999). "Fiber element for cyclic bending and shear of RC structures. I: Theory." *J. Eng. Mech.*, 10.1061/(ASCE)0733-9399(1999)125:9(994), 994-1001.

Popovics, S. (1973). "A numerical approach to the complete stress-strain curve of concrete." *Cement Concr. Res.*, 3(5), 583–599.

Portnov, G., Bakis, C. E., Lackey, E., and Kulakov, V. (2013). "FRP Reinforcing bars—designs and methods of manufacture (Review of Patents)." *Mech. Compos. Mater.*, 49(4), 381-400.

Ramirez, C. M. and Miranda, E. (2012). "Significance of residual drifts in building earthquake loss estimation." *Earthquake Eng. Struct. Dyn.*, 41(11), 1477-1493.

Santos, P., Laranja, G., França, P. M., and Correia, J. R. (2013). "Ductility and moment redistribution capacity of multi-span T-section concrete beams reinforced with GFRP bars." *Constr. Build. Mater.*, 49, 949-961.

Scott, B. D., Park, R., and Priestley, M. J. N. (1982). "Stress-strain behavior of concrete confined by overlapping hoops at low and high strain rates." *ACI Struct. J.*, 79(1), 13–27.

Seckin, M. (1981). "Hysteretic behaviour of cast-in-place exterior beam-column-slab subassemblies." Ph.D. dissertation, Dept. of Civil Engineering, Univ. of Toronto, Toronto, ON, Canada.

Sherstobitoff, J., Cajiao, P., and Adebar, P. (2012). "Analysis and repair of an earthquake-damaged high-rise building in Santiago, Chile." *15th World Conference on Earthquake Engineering*, Lisbon, Portugal.

Sritharan, S., Beyer, K., Henry, R. S., Chai, Y. H., Kowalsky, M., and Bull, D. (2014). "Understanding poor seismic performance of concrete walls and design implications." *Earthquake Spectra*, 30(1), 307-334.

Su, R. K. L., and Wong, S. M. (2007). "Seismic behaviour of slender reinforced concrete shear walls under high axial load ratio." *Eng. Struct.*, 29(8), 1957-1965.

Tavassoli, A. (2013). "Behaviour of GFRP-reinforced concrete columns under combined axial load and flexure." Master's thesis, Dept. of Civil and Environmental Engineering, Univ. of Toronto, ON, Canada.

Tobbi, H., Farghaly, A. S., and Benmokrane, B. (2012). "Concrete columns reinforced longitudinally and transversally with glass fiber-reinforced polymer bars." *ACI Struct. J.*, 109(4), 551.

Ulugtekin, D. (2010). "Analytical modeling of reinforced concrete panel elements under reversed cyclic loadings." M.A.Sc. thesis, Dept. of Civil Engineering, Bogazici Univ., Istanbul, Turkey.

Vecchio, F. J., and Collins, M. P. (1986). "The modified compression field theory for reinforced concrete elements subject to shear." *ACI Struct. J.*, 83(2), 219-231.

Vecchio, F. J. and McQuade, I. (2011). "Towards improved modeling of steel-concrete composite wall elements." *Nucl. Eng. Des.*, 241(8), 2629-42.

Vint, L. M. (2012). "Investigation of bond properties of glass fibre reinforced polymer bars in concrete under direct tension." Master's thesis, Dept. of Civil and Environmental Engineering, Univ. of Toronto, ON, Canada.

Wong, P. S., and Vecchio, F. J. (2002). "VecTor2 and formworks user's manual." *Technical Rep.*, Dept. of Civil Engineering, Univ. of Toronto, Toronto, ON, Canada.

Wong, P. S., and Vecchio, F. J., and Trommels, H. (2013). "VecTor2 and formworks user's manual, second edition." *Technical Rep.*, Dept. of Civil Engineering, Univ. of Toronto, Toronto, ON, Canada.

Yamakawa, T., and Fujisaki, T. (1995). "A study on elasto-plastic behavior of structural walls reinforced by CFRP grids." *Proc. of the Second Int. Symp. on Non-metallic (FRP) Reinforcement for Concrete Structures (FRPRCS-2), RILEM proc. 29*, 267–274.

Yamamoto, T. (1999). "Nonlinear finite element analysis of transverse shear and torsional problems in reinforced concrete shells," Master's thesis, Dept. of Civil Engineering, Univ. of Toronto, Toronto, ON, Canada.

Zhao, J., and Dun, H. (2014). "A restoring force model for steel fiber reinforced concrete shear walls." *Eng. Struct.*, 75, 469-476.